

Nonlinear Convective Instability of Turing-Unstable Fronts near Onset: A Case Study*

Anna Ghazaryan[†] and Björn Sandstede[‡]

Abstract. Fronts are traveling waves in spatially extended systems that connect two different spatially homogeneous rest states. If the rest state behind the front undergoes a supercritical Turing instability, then the front will also destabilize. On the linear level, however, the front will be only convectively unstable since perturbations will be pushed away from the front as it propagates. In other words, perturbations may grow, but they can do so only behind the front. The goal of this paper is to prove for a specific model system that this behavior carries over to the full nonlinear system.

Key words. fronts, Turing bifurcation, nonlinear stability, convective instability

AMS subject classifications. Primary, 37L15; Secondary, 35B32, 35B35, 35K45, 35K57, 37L10

DOI. 10.1137/060670262

1. Introduction. Propagating fronts are of interest in many different applications. In this manuscript, we are interested in the transition from stable to convectively unstable fronts: An initial perturbation to a convectively unstable front grows in time in any translation invariant norm but is simultaneously transported either to the right or to the left toward infinity in such a way that it decays pointwise at every fixed point in space as time goes to infinity [3]. It is worth pointing out that a convective instability can justifiably be viewed as a form of stability since perturbations decay pointwise: Consequently, we will use the terms “convective instability” and “convective stability” as synonyms. Whether or not an instability is convective depends strongly on the coordinate frame in which we measure the growth of perturbations. A natural reference frame for fronts is the comoving frame in which the front becomes stationary. Our aim is to show for a model system that the convective nature of certain front instabilities can be captured analytically.

The general situation can be described as follows. Consider a reaction-diffusion system

$$(1.1) \quad \partial_t U = D \partial_x^2 U + F(U; \alpha), \quad x \in \mathbb{R}, \quad t > 0, \quad U \in \mathbb{R}^N,$$

with a control parameter $\alpha \in \mathbb{R}$, where D is a diagonal matrix with strictly positive entries, and F is a smooth function. We assume that the system exhibits a front, i.e., a nonlinear wave $U(x, t) = U_h(x - ct)$ that travels with positive speed $c > 0$ and connects two different homogeneous rest states U_{\pm} so that $U_h(\xi) \rightarrow U_{\pm}$ as $\xi \rightarrow \pm\infty$. Once we specified that the

*Received by the editors September 19, 2006; accepted for publication by T. Kaper December 23, 2006; published electronically April 24, 2007. This work was supported by the NSF under grants DMS-9971703 and DMS-0203854.

<http://www.siam.org/journals/siads/6-2/67026.html>

[†]Department of Mathematics, University of North Carolina, Chapel Hill, NC 27599 (ghazarya@email.unc.edu).

[‡]Department of Mathematics, University of Surrey, Guildford, GU2 7XH, UK (b.sandstede@surrey.ac.uk). This author gratefully acknowledges a Royal Society Wolfson Research Merit Award.

front velocity c is positive so that the front travels toward $x = \infty$, we may refer to the rest states U_+ and U_- as being, respectively, ahead of and behind the front.

We say that a front is stable if every solution that starts near the front converges to the front, or one of its spatial translates, as time goes to infinity. A sufficient criterion for stability is that the spectrum of the linearization \mathcal{L} of (1.1) about the front, computed in the comoving frame $\xi = x - ct$, lies in the left half-plane except for a simple eigenvalue at the origin, which arises due to translational symmetry. Fronts become unstable when a subset of the spectrum of \mathcal{L} crosses the imaginary axis. The effect of such instabilities on the dynamics near a given front depends on which part of the spectrum crosses the imaginary axis. If isolated eigenvalues cross the imaginary axis, then the problem can be analyzed using Lyapunov–Schmidt reduction or, alternatively, center-manifold theory. The two generic bifurcations that occur are saddle-nodes and Hopf bifurcations. At a Hopf bifurcation, a unique modulated front bifurcates, i.e., a solution that becomes time periodic in an appropriate comoving coordinate frame. It is also possible that part of the essential spectrum crosses the imaginary axis. The boundary of the essential spectrum of \mathcal{L} coincides with the spectra of the asymptotic rest states U_{\pm} , and we concentrate here exclusively on Turing bifurcations of one of the asymptotic rest states: Turing bifurcations lead to stationary spatially periodic patterns whose deviation from the rest state is small; these patterns are commonly referred to as Turing patterns. If the rest state U_+ ahead of the front destabilizes, then there exists a continuum of modulated fronts which connect the rest state U_- behind the front with the Turing patterns ahead of the front [23]. The bifurcating modulated fronts are spectrally stable provided the periodic patterns are spectrally stable [22, 23]. For a certain model system that shares the main features of general reaction-diffusion systems, they have also been shown to be nonlinearly stable [10]. It should be emphasized that nonlinear stability does not follow from spectral stability, because the essential spectrum of the linearization about the modulated front touches the imaginary axis. The proof of nonlinear stability in [10] is based on exponential weights [4, 8, 9, 24] to handle the essential spectrum and on renormalization techniques [2, 7, 8] to take care of the nonlinearity.

In this paper, we are interested in the case where the rest state U_- behind the front destabilizes. It has been proved in [23] that modulated fronts that connect the Turing patterns behind the front to the rest state ahead cannot exist in this situation (see also [25] for related formal results). Thus, while the front is linearly unstable, there are no stable coherent front structures nearby. Numerical simulations and formal arguments give the following picture: The Turing bifurcation behind the front leads to stationary patterns. In the frame that moves with the front (which has speed c), we therefore expect, at least on the linear level, that initial perturbations to the front are transported with speed c to the left toward $x = -\infty$. In other words, the front can be thought of as pushing any perturbation away to the left. On the nonlinear level, we expect that growth saturates at the Turing pattern. Numerical simulations indeed show that initial data near the linearly unstable front evolve to a superposition of two fronts that move with different speeds, namely, a small Turing front which connects the Turing patterns far to the left with the unstable rest state U_- , and the primary linearly unstable front which travels faster and leaves the Turing front behind in its wake; see Figure 1. Sherratt [25] investigated in great detail the dynamics in the wake of convectively unstable fronts using formal arguments. Our goal is to make the above picture rigorous, at least for a model system similar to that considered in [10]: Our approach involves a priori estimates that we are

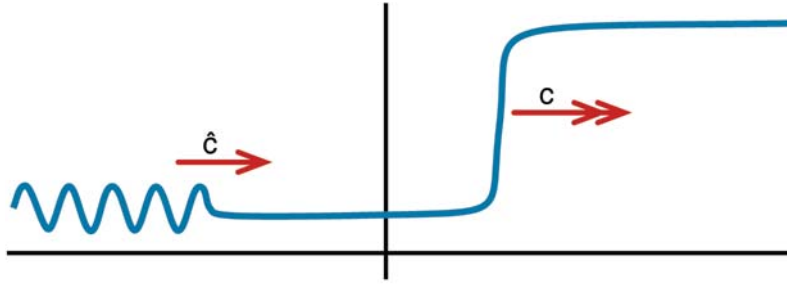


Figure 1. A schematic illustration of the expected dynamics near a convectively unstable front is shown. The speeds satisfy $\hat{c} < c$.

currently able to establish only in specific cases using restrictive tools such as the maximum principle and energy methods. We nevertheless believe that our general approach to nonlinear convective stability will apply more widely, which is why we carry out this case study. We certainly expect the overall phenomenon to be general for supercritical Turing bifurcations.

We consider the system

$$(1.2) \quad \begin{aligned} \partial_t u_1 &= \partial_x^2 u_1 + \frac{1}{2}(u_1 - c)(1 - u_1^2) + \gamma_1 u_2^2, \\ \partial_t u_2 &= -(1 + \partial_x^2)^2 u_2 + \alpha u_2 - u_2^3 - \gamma_2 u_2(1 + u_1), \end{aligned}$$

where $x \in \mathbb{R}$, $t \geq 0$, and $U = (u_1, u_2)$. The parameters $\gamma_1 \in \mathbb{R}$, $\gamma_2 > 0$, and $c \in (0, 1)$ are fixed, while the parameter α is a bifurcation parameter which varies near zero. For every α , the system (1.2) admits the traveling-wave solution

$$U_h(x - ct) = \begin{pmatrix} h(x - ct) \\ 0 \end{pmatrix}, \quad h(\xi) = \tanh \frac{\xi}{2},$$

which connects the rest state $U_- = (-1, 0)$ at $x = -\infty$ with the rest state $U_+ = (1, 0)$ at $x = \infty$. The idea of considering the Chafee–Infante equation coupled to the Swift–Hohenberg equation is adopted from [10], where a similar system has been used to investigate the nonlinear stability of modulated fronts which bifurcate when the rest state ahead of the primary front becomes unstable.

A standard bifurcation argument (see, for instance, [4]) has been used in [11] to show that spatially periodic equilibria bifurcate at $\alpha = 0$ from the rest state U_- . More precisely, assume that the parameters γ_1 and γ_2 satisfy

$$(1.3) \quad \gamma_1 \gamma_2 > -\frac{3(1+c)(5+c)}{11+3c};$$

then (1.2) has spatially periodic equilibria U_{per} for $\alpha > 0$ sufficiently close to zero which are given by

$$(1.4) \quad U_{\text{per}}(x) = \begin{pmatrix} -1 \\ 0 \end{pmatrix} + \sqrt{\frac{\alpha}{a_0}} \begin{pmatrix} 0 \\ \cos x \end{pmatrix} + O(\alpha), \quad a_0 = \frac{3}{4} + \frac{\gamma_1 \gamma_2}{2} \left(\frac{1}{1+c} + \frac{1}{2(5+c)} \right).$$

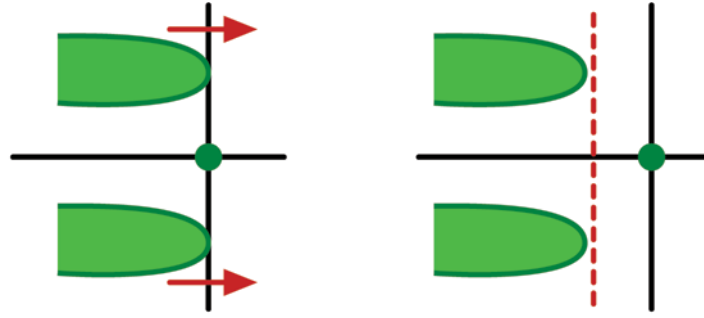


Figure 2. A schematic picture of the spectrum of the front U_h of (1.2) in the comoving frame $\xi = x - ct$ is shown in the complex plane \mathbb{C} for $\alpha = 0$ in spaces with (right) and without (left) exponential weight $e^{\beta\xi}$ with $\beta > 0$. Upon increasing α , the spectrum moves in the direction indicated by the arrows on spaces without exponential weights but stays to the left of the imaginary axis in spaces with exponential weight.

In particular, the bifurcation is supercritical provided (1.3) holds. The following result shows that the periodic patterns are nonlinearly stable with respect to perturbations in the space $H^2(2)$ defined to be the set of L^2 -functions for which the norm

$$\|U\|_{H^2(2)} := \left(\sum_{j=0}^2 \int_{\mathbb{R}} |\partial_x^j U(x)|^2 (1+x^2)^2 dx \right)^{\frac{1}{2}}$$

is finite.

Theorem 1 (see [11, Theorem 3.2]). *Assume that $\gamma_2 > 0$ and $c \in (0, 1)$ are fixed and that (1.3) is met. For each $\alpha > 0$ sufficiently small, there are positive numbers K and δ such that, for every $V_0 \in H^2(2)$ with $\|V_0\|_{H^2(2)} \leq \delta$, (1.2) with initial data $U_{\text{per}} + V_0$ has a unique global solution $U(t) = U_{\text{per}} + V(t)$, and $\|V(t)\|_{C^0} \leq K(1+t)^{-1/2}$ for $t \geq 0$.*

The proof of the preceding theorem is essentially identical to that of [10, Theorem 2.4], where a slightly different system was studied, and we therefore refer the reader to [11] for details.

The front U_h exists for all values of α but it will be spectrally unstable for $\alpha > 0$, since part of its essential spectrum will then lie in the open right half-plane. To repeat the reasoning outlined above, we might expect that waves bifurcating from the front at $\alpha = 0$ resemble a pattern obtained by gluing together the front U_h and the Turing patterns U_{per} that emerge in its wake. Such waves would be time-periodic, rather than stationary, in a frame that moves with the front. It was shown though in [23] that, for small $\alpha > 0$, such waves cannot bifurcate. Thus, it is natural to ask how perturbations of the front will evolve in time for $\alpha > 0$. We shall see that the spectrum of the front can actually be moved into the left half-plane in the comoving frame $\xi = x - ct$, provided it is computed in an exponentially weighted function space with norm $\|e^{\beta\xi}U(\xi)\|$ for some appropriate $\beta > 0$; see Figure 2 for an illustration. Thus, if perturbations are localized ahead of the front, while being allowed to grow behind the front, then they will decay exponentially in time as $t \rightarrow \infty$. The main result of this paper asserts that the same statement is true for the full nonlinear problem: The front is only convectively unstable for $\alpha > 0$ in that perturbations are pushed away from the front toward its wake.

The results on nonlinear convective instability of the front U_h are formulated in the spaces $H_{\text{ul}}^1(\mathbb{R}, \mathbb{R}^2)$ of uniformly local functions (see [16, section 3.1]) whose definition we recall in section 2. These spaces contain, in particular, all differentiable bounded functions such as fronts or periodic solutions. The results furthermore utilize the smooth weight functions

$$(1.5) \quad \rho_\beta(x) := \begin{cases} e^{\beta x}, & x \leq -1, \\ 1, & x \geq 1, \end{cases}$$

defined for $\beta > 0$, with $\rho'_\beta(x) \geq 0$ for all x .

Theorem 2. *Assume that $\gamma_2 > 0$ and $c \in (0, 1)$ are fixed, that (1.3) is met, and further that either $\gamma_1 \geq 0$ or else $\gamma_2 < \gamma_1 + \sqrt{2} < \sqrt{2}$. There are then positive constants α_* , β_* , ε_* , K , and Λ_* so that the following is true for all (α, ε) with $|\alpha| < \alpha_*$ and $0 < \varepsilon < \varepsilon_*$: For every function $V_0 = (v_1^0, v_2^0)$ with*

$$\|v_1^0\|_{H_{\text{ul}}^1} \leq \varepsilon^2, \quad \|v_2^0\|_{H_{\text{ul}}^1} \leq \varepsilon, \quad \|\rho_{\beta_*} V_0\|_{H_{\text{ul}}^1} \leq \varepsilon^2,$$

(1.2) with initial data $U_0 = U_h + V_0$ has a unique global solution $U(t)$, which can be expressed as

$$U(x, t) = U_h(x - ct - q(t)) + V(x, t)$$

for an appropriate real-valued function $q(t)$, and there is a $q_* \in \mathbb{R}$ so that

$$(1.6) \quad \|V(\cdot, t)\|_{H_{\text{ul}}^1} + |q(t)| \leq K \left[\varepsilon + \sqrt{|\alpha|} \right]^{\frac{1}{2}}, \quad \|\rho_{\beta_*}(\cdot - ct)V(\cdot, t)\|_{H_{\text{ul}}^1} + |q(t) - q_*| \leq K e^{-\Lambda_* t}$$

for $t \geq 0$.

Upon setting $\eta_* := \varepsilon_*^2/2$ and $K_* := K[\varepsilon_* + \sqrt{\alpha_*}]^{1/2}/\eta_*$, we obtain the following slightly weaker, but also less technical, corollary of Theorem 2 which we formulate in the comoving frame.

Corollary 1. *Under the assumptions of Theorem 2, there are positive constants α_* , β_* , η_* , K_* , and Λ_* so that the following is true for all α with $|\alpha| < \alpha_*$: For each function V_0 with $\|V_0\|_{H_{\text{ul}}^1} \leq \eta_*$, (1.2) with initial data $U_0 = U_h + V_0$ has a unique global solution $U(t)$, which can be expressed as*

$$U(x, t) = U_h(x - ct - q(t)) + V(x - ct, t)$$

for an appropriate real-valued function $q(t)$, and there is a $q_* \in \mathbb{R}$ so that

$$\|V(\cdot, t)\|_{H_{\text{ul}}^1} + |q(t)| \leq K_* \eta_*, \quad \|\rho_{\beta_*}(\cdot)V(\cdot, t)\|_{H_{\text{ul}}^1} + |q(t) - q_*| \leq K_* e^{-\Lambda_* t}$$

for $t \geq 0$.

Thus, the conclusion of the preceding theorem and corollary is that the dynamical behavior of the front does not change at all near $\alpha = 0$ provided we measure perturbations in the weighted norm: Perturbations stay bounded in the C^0 -norm and decay exponentially to zero as $t \rightarrow \infty$ when they are multiplied by $e^{\beta_*(x-ct)}$ for some appropriate $\beta_* > 0$, so that the front is nonlinearly stable in this norm for all values of α near zero. Note that our results say nothing about the detailed dynamics behind the front. Indeed, our approach, outlined in

detail below, relies only on a priori estimates and does not take the specific dynamics behind the front into account.

We comment briefly on the scalings in ε and α that appear in Theorem 2. The components v_1 and v_2 of the perturbation V scale with different powers in ε because the instability manifests itself on a linear level only in the v_2 -component, while the v_1 -component is affected only through the quadratic nonlinearity. The estimates (1.6) for the perturbation V are certainly not optimal as we expect solutions to saturate at order $|\alpha|^{\frac{1}{2}}$. The weaker estimates (1.6) are an artifact of our method which requires a supercritical bifurcation, but not necessarily its genericity, and which consequently will not yield sharp estimates.

As already mentioned, nonlinear stability of the front U_h in the weighted spaces cannot be inferred from spectral stability because the nonlinearity does not map the weighted spaces into themselves. Indeed, if we define $W = e^{\beta x}V$ and use $W = (w_1, w_2)$ as the new dependent variable, then we would like to find bounds for W in C^0 or H_{ul}^1 . If we transform the equation for the initial perturbation V to the new weighted variable W , then the nonlinear term u_1^n becomes

$$e^{\beta x} [e^{-\beta x} w_1]^n = e^{(1-n)\beta x} w_1^n,$$

which is unbounded as $x \rightarrow -\infty$ for $n > 1$. To overcome this difficulty, we use a method introduced originally in [19] in the Hamiltonian context. If we can obtain a priori estimates for the solution in the space without weight, for instance, in C^0 or H_{ul}^1 , and show that it stays bounded and sufficiently small, then the nonlinear terms u_j^n , written as $u_j^n = u_j^{n-1}u_j$, become $u_j^{n-1}w_j$ when transformed to the weighted functions W , which are now well behaved due to the a priori estimates for u_j . This interplay of the spatially uniform norm and the exponentially weighted norm is the key for the proof of nonlinear stability of the front. An example of a successful application of this technique has also been given independently in [1], where a reaction-diffusion-convection system is considered that has essential spectra up to the imaginary axis for all values of the bifurcation parameter while an isolated pair of simple eigenvalues crosses the imaginary axis at the bifurcation point.

The plan of the paper is as follows. In section 2, we discuss the spectral stability of the front and state several auxiliary results that we need later. Section 3 contains the proof of Theorem 2. Numerical simulations and some further implications of our results are given in section 4, and we end with conclusions and a discussion in section 5.

2. Linear convective instability. We begin by introducing the spaces $L_{\text{ul}}^2(\mathbb{R})$ from [16] in which we shall work. Pick any positive and bounded function $\sigma \in C^2(\mathbb{R})$ for which $\int_{\mathbb{R}} \sigma(x) dx = 1$ and $|\sigma'(x)|, |\sigma''(x)| \leq \sigma(x)$ for $x \in \mathbb{R}$: We may, for instance, set $\sigma(x) = \frac{1}{\pi} \operatorname{sech} x$. For each $0 < b < 1$, we define $\sigma_b(x) := \sigma(bx)$ and record that $\int_{\mathbb{R}} \sigma_b(x) dx = 1/b$.

Using the weight function σ , we define the Banach space L_{ul}^2 of uniformly local weighted L^2 functions to be

$$L_{\text{ul}}^2(\mathbb{R}) = \left\{ u \in L_{\text{loc}}^2(\mathbb{R}) : \|u\|_{L_{\text{ul}}^2}^2 := \sup_{y \in \mathbb{R}} \int_{\mathbb{R}} \sigma(x+y) |u(x)|^2 dx < \infty \right. \\ \left. \text{and } \|T_y u - u\|_{L_{\text{ul}}^2} \rightarrow 0 \text{ as } y \rightarrow 0 \right\},$$

where $[T_y u](x) := u(x + y)$ is the translation operator. We denote the associated Sobolev spaces by $H_{\text{ul}}^k(\mathbb{R})$ and remark that different choices for σ result in the same spaces with equivalent norms. We collect various properties of these spaces in the following lemma.

Lemma 2.1 (see [16, Lemmas 3.1 and 3.8]). *There is a constant K_0 with the following properties:*

- (i) H_{ul}^1 is an algebra and embeds continuously into C_{unif}^0 with $\|u\|_{C^0}^2 \leq K_0 \|u\|_{L_{\text{ul}}^2} \|u\|_{H_{\text{ul}}^1}$ for all $u \in H_{\text{ul}}^1$.
- (ii) For each $0 < b < 1$, let $\sigma_b(x) := \sigma(bx)$; then $\|u\|_{L_{\text{ul}}^2(\sigma)}^2 \leq K_0(1 + b) \|u\|_{L_{\text{ul}}^2(\sigma_b)}^2$ for all $u \in L_{\text{ul}}^2(\sigma)$.
- (iii) We have $-\int_{\mathbb{R}} \sigma_b u (1 + \partial_x^2)^2 u \, dx \leq \frac{7b^2}{2} \int_{\mathbb{R}} \sigma_b u^2 \, dx$ for all $u \in H_{\text{ul}}^4$.

We return now to the partial differential equation (1.2). Upon transforming (1.2) into the comoving coordinate $\xi = x - ct$, we obtain the system

$$(2.1) \quad \begin{aligned} \partial_t u_1 &= \partial_\xi^2 u_1 + c \partial_\xi u_1 + \frac{1}{2}(u_1 - c)(1 - u_1^2) + \gamma_1 u_2^2, \\ \partial_t u_2 &= -(1 + \partial_\xi^2)^2 u_2 + c \partial_\xi u_2 + \alpha u_2 - u_2^3 - \gamma_2 u_2(1 + u_1). \end{aligned}$$

The linearization of (2.1) about a stationary solution of the form $U_* = (u_*, 0)$ is given by the diagonal operator

$$(2.2) \quad \mathcal{L}_0[U_*] := \begin{pmatrix} \partial_\xi^2 + c \partial_\xi + \frac{1}{2}(1 + 2cu_* - 3u_*^2) & 0 \\ 0 & -[1 + \partial_\xi^2]^2 + c \partial_\xi + \alpha - \gamma_2(1 + u_*) \end{pmatrix}.$$

The operator $\mathcal{L}_0[U_*]$ is sectorial on $\mathcal{X}_0 := H_{\text{ul}}^1 \times H_{\text{ul}}^1$ with dense domain $H_{\text{ul}}^3 \times H_{\text{ul}}^5$. We shall also consider (2.2) in exponentially weighted spaces: For $\beta > 0$, we defined in (1.5) the weight function

$$\rho_\beta(\xi) = \begin{cases} e^{\beta\xi}, & \xi \leq -1, \\ 1, & \xi \geq 1, \end{cases}$$

where $\rho'_\beta(\xi) \geq 0$ for all ξ . We then set

$$W(\xi) := \rho_\beta(\xi)V(\xi)$$

so that W satisfies $W_t = \mathcal{L}_\beta[U_*]W$ with

$$\mathcal{L}_\beta[U_*] = \rho_\beta \mathcal{L}_0[U_*] \rho_\beta^{-1}$$

whenever V satisfies $V_t = \mathcal{L}_0[U_*]V$. It is easy to check that the operator $\mathcal{L}_\beta[U_*]$ is again sectorial on \mathcal{X}_0 . From now on, we shall denote by $\mathcal{L}_\beta := \mathcal{L}_\beta[U_h]$ the linearized operator belonging to the front U_h .

Proposition 2.2. *Given $\gamma_2 > 0$ and $c \in (0, 1)$, there are positive numbers α_0 and β_0 and a strictly positive function $\Lambda_0(\beta)$ defined for $0 < \beta < \beta_0$ so that the following holds for $|\alpha| \leq \alpha_0$: The spectrum of \mathcal{L}_β satisfies*

$$\text{spec}(\mathcal{L}_\beta) = \{0\} \cup \Sigma \quad \text{with} \quad \text{Re } \Sigma \leq -\Lambda_0(\beta),$$

and $\lambda = 0$ is the simple eigenvalue of \mathcal{L}_β and \mathcal{L}_0 . Furthermore, the spectrum of \mathcal{L}_0 satisfies

$$\begin{aligned} \operatorname{spec}(\mathcal{L}_0) &= \{0\} \cup \Sigma \text{ with } \operatorname{Re} \Sigma < 0 \text{ for } \alpha < 0, \\ \operatorname{spec}(\mathcal{L}_0) \cap \{\lambda : \operatorname{Re} \lambda \geq 0\} &= \{0\} \cup \{\pm i\} \text{ for } \alpha = 0, \end{aligned}$$

and $\operatorname{spec}(\mathcal{L}_0) \cap \{\lambda : \operatorname{Re} \lambda > 0\} \neq \emptyset$ for $\alpha > 0$.

In particular, the front U_h is orbitally stable for $\alpha < 0$ due to [12, section 5.1], while it is spectrally unstable for $\alpha > 0$.

Proof. For each β , the spectrum of \mathcal{L}_β on \mathcal{X}_0 is the disjoint union of the essential spectrum and the point spectrum, where the latter consists, by definition, of all isolated eigenvalues with finite multiplicity. It follows from [12, appendix to section 5] or [17] that the essential spectrum of \mathcal{L}_β on \mathcal{X}_0 is, for any $\beta \geq 0$, bounded to the right by the essential spectra of the asymptotic operators

$$\mathcal{L}_\beta^- := \mathcal{L}_\beta[U_-] = \begin{pmatrix} (\partial_\xi - \beta)^2 + c(\partial_\xi - \beta) - (1 + c) & 0 \\ 0 & -[1 + (\partial_\xi - \beta)^2]^2 + c(\partial_\xi - \beta) + \alpha \end{pmatrix}$$

and $\mathcal{L}_0^+ := \mathcal{L}_0[U_+]$. Indeed, the weight function ρ_β is equal to one for $\xi \geq 1$ and therefore has no effect on the asymptotic coefficients when $\xi \rightarrow \infty$.

Thus, to determine the rightmost elements in the essential spectrum of \mathcal{L}_0 , it suffices to compute the essential spectra of the operators \mathcal{L}_0^\pm on the space \mathcal{X}_0 . On account of multiplier theory [16, Lemma 3.3], these spectra can be calculated using the Fourier transform: A complex number λ is in the spectrum of \mathcal{L}_0^\pm if and only if there are a vector $V_0 \in \mathbb{C}^2$ and a number $k \in \mathbb{R}$ so that

$$\lambda e^{ik\xi} V_0 = \mathcal{L}_0^\pm e^{ik\xi} V_0,$$

that is, if and only if

$$\det \begin{pmatrix} -k^2 + ikc + \frac{1}{2}(1 + 2cu_\pm - 3u_\pm^2) - \lambda & 0 \\ 0 & -(1 - k^2)^2 + ikc + \alpha - \gamma_2(1 + u_\pm) - \lambda \end{pmatrix} = 0,$$

where $u_\pm = \pm 1$. In particular, we see that the spectrum of \mathcal{L}_0^+ is given by

$$\begin{aligned} \operatorname{spec}(\mathcal{L}_0^+) &= \{\lambda \in \mathbb{C}; \lambda = \lambda_1^+(k) := -k^2 + ikc - (1 - c) \text{ or} \\ &\quad \lambda = \lambda_2^+(k) := -(1 - k^2)^2 + ikc + \alpha - 2\gamma_2 \text{ for some } k \in \mathbb{R}\} \end{aligned}$$

and therefore lies in the left half-plane and is uniformly bounded away from the imaginary axis for all α near zero. Similarly, the spectrum of the operator \mathcal{L}_0^- associated with the rest state behind the front is given by

$$(2.3) \quad \begin{aligned} \operatorname{spec}(\mathcal{L}_0^-) &= \{\lambda \in \mathbb{C}; \lambda = \lambda_1^-(k) := -k^2 + ikc - (1 + c) \text{ or} \\ &\quad \lambda = \lambda_2^-(k) := -(1 - k^2)^2 + ikc + \alpha \text{ for some } k \in \mathbb{R}\}. \end{aligned}$$

It lies in the left half-plane, bounded away from the imaginary axis, except for the curve $\lambda = \lambda_2^-(k)$ which crosses into the right half-plane for $\alpha \geq 0$ and $k \in \mathbb{R}$ near $k_c = \pm 1$.

The spectrum of \mathcal{L}_β^- can be computed either analogously or, more directly, by replacing k with $k + i\beta$ in the above expression for $\text{spec}(\mathcal{L}_0^-)$. The rightmost part of the spectrum of \mathcal{L}_β^- is therefore given by the linear dispersion curve

$$\lambda = \lambda_2^-(k + i\beta) = -(1 - k^2 + \beta^2)^2 + \alpha - c\beta + 4\beta^2 k^2 + i[ck - 4\beta k(1 - k^2 - \beta^2)]$$

for $k \in \mathbb{R}$, and we have

$$(2.4) \quad \max_{k \in \mathbb{R}} \text{Re } \lambda_2^-(k + i\beta) = \alpha - c\beta + 4\beta^2(1 + 2\beta^2),$$

which is achieved at $k = \pm\sqrt{1 + 3\beta^2}$. Choosing $\beta = \frac{c}{8}$, we obtain the bound

$$\Lambda_{\text{ess}}^- = \alpha - \frac{c^2}{16} \left(1 - \frac{c^2}{32}\right) < 0$$

for the maximal real part of $\text{spec}(\mathcal{L}_\beta^-)$, which is strictly negative for fixed $c \in (0, 1)$ and $|\alpha| \leq \frac{c^2}{32}$.

In summary, the essential spectrum of \mathcal{L}_0 lies in the open left half-plane for $\alpha = 0$, touches the imaginary axis at $\lambda = \pm i$ when $\alpha = 0$, and crosses into the right half-plane for $\alpha > 0$.

Having discussed the essential spectrum, we now turn to the point spectrum. The situation here is similar to the one considered in [10]. The eigenfunctions associated with isolated eigenvalues of \mathcal{L}_0 necessarily decay exponentially as $|\xi| \rightarrow \infty$. The origin $\lambda = 0$ is always in the point spectrum of \mathcal{L}_0 with eigenfunction $U'_h(\xi) = (h_\xi(\xi), 0)$.

For $\alpha < 0$, any isolated eigenvalue λ of \mathcal{L}_0 satisfies either $\text{Re } \lambda < 0$ or $\lambda = 0$. To prove this claim, we assume that there is an eigenvalue λ with eigenfunction $V = (v_1, v_2)$ which therefore satisfies the decoupled system

$$(2.5) \quad \lambda v_1 = \partial_\xi^2 v_1 + c\partial_\xi v_1 + \frac{1}{2}(1 + 2ch - 3h^2)v_1,$$

$$(2.6) \quad \lambda v_2 = -(1 + \partial_\xi^2)^2 v_2 + c\partial_\xi v_2 + \alpha v_2 - \gamma_2(1 + h)v_2.$$

We see that $\lambda = 0$ is an eigenvalue of (2.5) with positive eigenfunction $h_\xi(\xi) = \frac{1}{2} \text{sech}^2 \frac{\xi}{2}$. Sturm–Liouville theory implies that $\lambda = 0$ is simple for (2.5) and that all other eigenvalues of (2.5) are strictly negative. To analyze (2.6), we multiply by \bar{v}_2 and integrate over \mathbb{R} to obtain

$$\text{Re } \lambda \|v_2\|_{L^2}^2 \leq -\|(1 + \partial_\xi^2)v_2\|_{L^2}^2 + \alpha \|v_2\|_{L^2}^2 \leq \alpha \|v_2\|_{L^2}^2,$$

where we used that $\gamma_2(1 + h(\xi)) \geq 0$. Thus, either $\text{Re } \lambda \leq \alpha$ or $v_2 = 0$, which proves the claim.

Next, we consider the isolated eigenvalues of \mathcal{L}_β for $0 < \beta < \beta_0$ for an appropriate $\beta_0 > 0$. We claim that there are no eigenvalues on or to the right of the imaginary axis for all α with $|\alpha|$ sufficiently small, except for a simple eigenvalue at the origin. To prove this claim, we first record that eigenfunctions associated with isolated eigenvalues of \mathcal{L}_β in the closed right half-plane decay exponentially as $\xi \rightarrow \infty$ with a rate that does not depend on the eigenvalue. In particular, there is a $\beta_0 > 0$ so that the following is true for each $0 < \beta \leq \beta_0$: if $(w_1, w_2) = \rho_\beta(v_1, v_2)$ is an L^2 -eigenfunction of \mathcal{L}_β belonging to an eigenvalue λ

with $\operatorname{Re} \lambda \geq 0$, then $e^{\beta\xi}(v_1, v_2)$ will also be in L^2 . Thus, it suffices to prove the claim for the operator $e^{\beta\xi}\mathcal{L}_0(\partial_\xi)e^{-\beta\xi} = \mathcal{L}_0(\partial_\xi - \beta)$: the associated eigenvalue problem is given by

$$(2.7) \quad \lambda w_1 = (\partial_\xi - \beta)^2 w_1 + c(\partial_\xi - \beta)w_1 + \frac{1}{2}(1 + 2ch - 3h^2)w_1,$$

$$(2.8) \quad \lambda w_2 = -(1 + (\partial_\xi - \beta)^2)w_2 + c(\partial_\xi - \beta)w_2 + \alpha w_2 - \gamma_2(1 + h)w_2.$$

Multiplying (2.8) by \bar{w}_2 and integrating over \mathbb{R} , we obtain

$$\operatorname{Re} \lambda \|w_2\|_{L^2} \leq (\alpha - c\beta) \|w_2\|_{L^2} \leq 0,$$

and therefore either $\operatorname{Re} \lambda \leq \alpha - c\beta < 0$ or $w_2 = 0$. It remains to consider (2.7), which has an eigenvalue at the origin with bounded positive eigenfunction $e^{\beta\xi}h_\xi(\xi)$. Sturm–Liouville theory implies again that all other eigenvalues are strictly negative: In fact, the largest negative eigenvalue is equal to $-\frac{3}{4}(1 - c^2)$. Thus, for eigenvalues λ of (2.7)–(2.8), we have $\lambda = 0$ or $\operatorname{Re} \lambda \leq \max\{\alpha - c\beta, -\frac{3}{4}(1 - c^2)\} < 0$, and as mentioned above the same statement holds for the eigenvalues of \mathcal{L}_β .

Finally, we remark that solutions V of (2.5)–(2.6) and W of (2.7)–(2.8) are in one-to-one correspondence via $W(\xi) = e^{\beta\xi}V(\xi)$. This shows that \mathcal{L}_0 cannot have any isolated eigenvalues in the closed right half-plane except at $\lambda = 0$. ■

In the nonlinear stability analysis of our model, we need the semigroup estimates for the operators

$$\mathcal{A}_1 := \partial_x^2 - (1 + c), \quad \mathcal{A}_2 := -(1 + \partial_x^2)^2$$

provided by the following lemma, which is a straightforward application of multiplier theory [16, Lemma 3.3].

Lemma 2.3. *The operators \mathcal{A}_1 and \mathcal{A}_2 are sectorial and thus generate holomorphic semigroups $e^{\mathcal{A}_1 t}$ and $e^{\mathcal{A}_2 t}$. There is a positive constant K_0 with*

$$\begin{aligned} \|e^{\mathcal{A}_1 t}\|_{L_{\text{ul}}^2 \rightarrow H_{\text{ul}}^1} &\leq K_0(1 + t^{-\frac{1}{4}})e^{-t}, & \|e^{\mathcal{A}_1 t}\|_{H_{\text{ul}}^1 \rightarrow H_{\text{ul}}^1} &\leq K_0 e^{-t}, \\ \|e^{\mathcal{A}_2 t}\|_{L_{\text{ul}}^2 \rightarrow H_{\text{ul}}^s} &\leq K_0(1 + t^{-\frac{s}{4}}), & \|e^{\mathcal{A}_2 t}\|_{H_{\text{ul}}^1 \rightarrow H_{\text{ul}}^1} &\leq K_0 \end{aligned}$$

uniformly in $t > 0$.

3. Nonlinear convective instability. This section contains the proof of Theorem 2. We want to show that the front is convectively stable in the comoving frame for initial perturbations which are small in H_{ul}^1 . In the comoving frame $\xi = x - ct$, the front is a stationary solution of

$$(3.1) \quad \begin{aligned} \partial_t u_1 &= \partial_\xi^2 u_1 + c\partial_\xi u_1 + \frac{1}{2}(u_1 - c)(1 - u_1^2) + \gamma_1 u_2^2, \\ \partial_t u_2 &= -(1 + \partial_\xi^2)^2 u_2 + c\partial_\xi u_2 + \alpha u_2 - u_2^3 - \gamma_2 u_2(1 + u_1). \end{aligned}$$

The proof of Theorem 2 is divided into two parts. First we show that suitable a priori estimates imply the nonlinear stability of the front in appropriate exponentially weighted norms imposed in the comoving frame. Afterward, we establish these a priori estimates. We focus exclusively on the case $\gamma_1 \geq 0$ and refer the reader to [11] for the modifications that are necessary for the case $\gamma_2 < \gamma_1 + \sqrt{2} < \sqrt{2}$. Recall that $\gamma_2 > 0$ and $c \in (0, 1)$ are both fixed.

3.1. A priori estimates imply nonlinear stability. We expect that initial data close to the front will converge to an appropriate translate of the front but not necessarily to the primary front U_h itself. To capture this behavior, we introduce a time-dependent spatial shift function $q(t)$ in the argument of the front U_h and write solutions to (3.1) as

$$(3.2) \quad U(\xi, t) = \begin{pmatrix} u_1(\xi, t) \\ u_2(\xi, t) \end{pmatrix} = \begin{pmatrix} h(\xi - q(t)) \\ 0 \end{pmatrix} + \begin{pmatrix} v_1(\xi, t) \\ v_2(\xi, t) \end{pmatrix},$$

with $h(\xi) = \tanh \frac{\xi}{2}$. We may assume that $q(0) = 0$ since our system is translationally invariant. The decomposition (3.2) can be made unique by requiring that the perturbation $V = (v_1, v_2)$ be “perpendicular,” in an appropriate way that we specify below, to the one-dimensional subspace spanned by the derivative of the front.

The perturbation $V = (v_1, v_2)$ of the front satisfies the system

$$(3.3) \quad \begin{aligned} \partial_t v_1 &= \partial_\xi^2 v_1 + c \partial_\xi v_1 + \frac{1}{2} [1 - 3h^2(\xi - q(t)) + 2ch(\xi - q(t))] v_1 + \frac{1}{2} [c - 3h(\xi - q(t))] v_1^2 \\ &\quad - \frac{1}{2} v_1^3 + \dot{q}(t) h_\xi(\xi - q(t)) + \gamma_1 v_2^2, \\ \partial_t v_2 &= -(1 + \partial_\xi^2) v_2 + c \partial_\xi v_2 + \alpha v_2 - v_2^3 - \gamma_2 (1 + h(\xi - q(t))) v_2 - \gamma_2 v_1 v_2 \end{aligned}$$

with initial data $v_1(\xi, 0) = v_1^0(\xi)$, $v_2(\xi, 0) = v_2^0(\xi)$, and $q(0) = 0$. Using the notation

$$\begin{aligned} \mathcal{A} &= \begin{pmatrix} \partial_\xi^2 + c \partial_\xi & 0 \\ 0 & -(1 + \partial_\xi^2)^2 + c \partial_\xi + \alpha \end{pmatrix}, \\ \mathcal{R}(\xi) &= \begin{pmatrix} \mathcal{R}_1 & 0 \\ 0 & \mathcal{R}_2 \end{pmatrix} = \begin{pmatrix} \frac{1}{2} [1 - 3h^2(\xi) + 2ch(\xi)] & 0 \\ 0 & -\gamma_2 (1 + h(\xi)) \end{pmatrix}, \\ \mathcal{N}(V) &= \begin{pmatrix} \mathcal{N}_1(V) \\ \mathcal{N}_2(V) \end{pmatrix} = \begin{pmatrix} \frac{1}{2} [c - 3h(\xi - q(t))] v_1(\xi, t) - \frac{1}{2} v_1^2(\xi, t) & \gamma_1 v_2(\xi, t) \\ 0 & -v_2^2(\xi, t) - \gamma_2 v_1(\xi, t) \end{pmatrix}, \end{aligned}$$

system (3.3) becomes

$$(3.4) \quad \partial_t V = \mathcal{A}V + \mathcal{R}(\xi - q(t))V + \mathcal{N}(V)V + \dot{q}(t)h_\xi(\xi - q(t))e_1, \quad e_1 = (1, 0).$$

Next, we introduce the weighted solution $W = (w_1, w_2)$ via

$$W(\xi, t) = \rho_\beta(\xi)V(\xi, t),$$

with ρ_β as defined in (1.5), which satisfies the system

$$(3.5) \quad \partial_t W = \mathcal{L}_\beta W + [\mathcal{R}(\xi - q(t)) - \mathcal{R}(\xi)]W + \mathcal{N}(V)W + \dot{q}(t)h_\xi(\xi - q(t))\rho_\beta(\xi)e_1$$

with $\mathcal{L}_\beta = \rho_\beta \mathcal{A} \rho_\beta^{-1} + \mathcal{R}(\xi)$ being the linearization of the front U_h discussed in section 2 whenever $V(\xi, t)$ satisfies (3.4).

Throughout the remainder of the proof, we fix β with $0 < \beta < \beta_0$ as in Proposition 2.2: We then know that $\lambda = 0$ is a simple isolated eigenvalue of \mathcal{L}_β with eigenfunction $\rho_\beta(\xi)\partial_\xi U_h$ and the rest of the spectrum has real part less than Λ_0 with Λ_0 from Proposition 2.2. We define

$\mathcal{P}_\beta^c : H_{\text{ul}}^1 \times H_{\text{ul}}^1 \rightarrow H_{\text{ul}}^1 \times H_{\text{ul}}^1$ to be the spectral projection onto the one-dimensional eigenspace of \mathcal{L}_β corresponding to the zero eigenvalue and denote by $\mathcal{P}_\beta^s = 1 - \mathcal{P}_\beta^c$ the complementary projection onto the stable eigenspace.

Lemma 3.1. *For $0 < \beta < \beta_0$, there are constants $K_0 > 0$ and $\alpha_0 > 0$ such that the following is true for any α with $|\alpha| < \alpha_0$. The spectral projection \mathcal{P}_β^c is given by*

$$(3.6) \quad \mathcal{P}_\beta^c W = \begin{pmatrix} P_\beta^c & 0 \\ 0 & 0 \end{pmatrix} W = \langle \psi_1^c, W_1 \rangle_{L^2} \rho_\beta \partial_\xi U_h,$$

where

$$\psi_1^c(\xi) = \frac{e^{c\xi} \rho_\beta(\xi) h_\xi(\xi)}{\int_{\mathbb{R}} e^{c\xi} h_\xi(\xi)^2 d\xi},$$

and we have

$$(3.7) \quad \|e^{\mathcal{P}_\beta^c \mathcal{L}_\beta t}\|_{H_{\text{ul}}^1} \leq K_0 e^{-\Lambda_0 t}, \quad t \geq 0,$$

with Λ_0 as in Proposition 2.2.

Proof. It is easy to check that, in the space of bounded functions, the kernel of the operator adjoint to \mathcal{L}_β is spanned by $(h_\xi(\xi) e^{c\xi} \rho_\beta(\xi), 0)$. Upon normalizing this function, we end up with the expression (3.6) for the center projection. The estimate (3.7) is a consequence of Proposition 2.2 once we observe that the constant K_0 does not depend on α despite the presence of α in the definition of \mathcal{L}_β . Indeed, when $\alpha = 0$, the spectrum of $\mathcal{P}_\beta^c \mathcal{L}_\beta$ belongs to $\{\lambda \in \mathbb{C} : \text{Re } \lambda < -\beta c\}$, and an estimate of the form (3.7) holds for some K_0 . The operator for $\alpha \neq 0$ is a bounded perturbation of order $O(\alpha)$ of the $\alpha = 0$ operator, and [18, Theorem 1.1] implies that K_0 can be chosen to be independent of α for α sufficiently close to zero. ■

To fix $q(t)$, we require that $\mathcal{P}_\beta^c W(t) = 0$ for all t for which the decomposition (3.2) exists. In other words, we require that $W(t) \in \text{Range}(\mathcal{P}_\beta^s)$ for all t . Applying the projections \mathcal{P}_β^c and \mathcal{P}_β^s to (3.5), we obtain the evolution system

$$(3.8) \quad \partial_t V = \mathcal{A}V + \mathcal{R}(\xi - q(t))V + \mathcal{N}(V)V + \dot{q}(t)h_\xi(\xi - q(t))e_1,$$

$$(3.9) \quad \partial_t W = \mathcal{P}_\beta^s \mathcal{L}_\beta W + \mathcal{P}_\beta^s ([\mathcal{R}(\xi - q(t)) - \mathcal{R}(\xi)]W + \mathcal{N}(V)W + \dot{q}(t)h_\xi(\xi - q(t))\rho_\beta(\xi)e_1),$$

$$(3.10) \quad \dot{q}(t) = -\frac{\langle \psi_1^c, [\mathcal{R}_1(\xi - q(t)) - \mathcal{R}_1(\xi)]W_1 + \mathcal{N}_1(V)W \rangle_{L^2}}{\langle \psi_1^c, h_\xi(\xi - q(t))\rho_\beta(\xi) \rangle_{L^2}}$$

for $V = (v_1, v_2)$, $W = (w_1, w_2)$, and q . It is easy to see that the linear parts of the right-hand sides in (3.8)–(3.9) are sectorial operators on $H_{\text{ul}}^1(\mathbb{R}, \mathbb{R}^2)$ with dense domain $H_{\text{ul}}^3 \times H_{\text{ul}}^5$. The nonlinearity is smooth from $\mathcal{Y} := H_{\text{ul}}^1(\mathbb{R}, \mathbb{R}^2) \times H_{\text{ul}}^1(\mathbb{R}, \mathbb{R}^2) \times \mathbb{R}$ into itself, and there is a constant K_1 such that

$$(3.11) \quad \|\mathcal{R}_1(\cdot - q) - \mathcal{R}_1(\cdot)\|_{H_{\text{ul}}^1} + \|\mathcal{N}(V)\|_{H_{\text{ul}}^1} \leq K_1(|q| + \|V\|_{H_{\text{ul}}^1})$$

and

$$(3.12) \quad |\dot{q}| \leq K_1(|q| + \|V\|_{H_{\text{ul}}^1})\|W\|_{H_{\text{ul}}^1}$$

for all $(V, W, q) \in \mathcal{Y}$ with norm less than one, say. We therefore have the methods introduced in [12] at our disposal which give local existence and uniqueness of solutions for initial data in \mathcal{Y} as well as continuous dependence on initial conditions, thus proving local existence and uniqueness of the decomposition (3.2).

These arguments also allow us to claim that, for each given $0 < \eta_0 \leq 1$, there exist a $\delta_0 > 0$ and a time $T > 0$ such that the decomposition (3.2) exists for $0 \leq t < T$ with

$$(3.13) \quad |q(t)| + \|V(t)\|_{H_{\text{ul}}^1} \leq \eta_0$$

provided $\|V(0)\|_{H_{\text{ul}}^1} \leq \delta_0$. Let $T_{\text{max}} = T_{\text{max}}(\eta_0)$ be the maximal time for which (3.13) holds.

Lemma 3.2. *Pick Λ with $0 < \Lambda < \Lambda_0$ and $\hat{\eta}_0 > 0$ so that*

$$(3.14) \quad \frac{2K_0K_1(1 + K_0)}{\Lambda_0 - \Lambda} \hat{\eta}_0 < 1;$$

then there are positive constants K_2 and K_3 that are independent of α such that for any $0 < \eta_0 \leq \hat{\eta}_0$ we have

$$\|W(t)\|_{H_{\text{ul}}^1} \leq K_2 e^{-\Lambda t} \|W(0)\|_{H_{\text{ul}}^1}, \quad |q(t)| \leq K_3 \|W(0)\|_{H_{\text{ul}}^1}$$

for all $0 \leq t < T_{\text{max}}(\eta_0)$ and any solution that satisfies (3.13). If $T_{\text{max}}(\eta_0) = \infty$, then there is a $q_ \in \mathbb{R}$ with*

$$(3.15) \quad |q(t) - q_*| \leq \frac{K_1 K_2}{\Lambda} e^{-\Lambda t} \|W(0)\|_{H_{\text{ul}}^1}$$

for $t \geq 0$.

Thus, to complete the proof of Theorem 2 once the lemma has been proved, it suffices to establish a priori estimates which guarantee that $V(t)$ stays so small that $T_{\text{max}} = \infty$ for our particular choice (3.14) of $\hat{\eta}_0$.

Proof. The variation-of-constants formula applied to (3.9) gives

$$W(t) = e^{\mathcal{P}_\beta^s \mathcal{L}_\beta t} W(0) + \int_0^t e^{\mathcal{P}_\beta^s \mathcal{L}_\beta (t-s)} \mathcal{P}_\beta^s [(\mathcal{R}(\xi - q(s)) - \mathcal{R}(\xi) + \mathcal{N}(V(s))) W(s) + \dot{q}(s) h_\xi(\xi - q(s)) \rho_\beta(\xi) e_1] ds.$$

The estimates (3.7) and (3.11) give

$$\|W(t)\|_{H_{\text{ul}}^1} \leq K_0 e^{-\Lambda_0 t} \|W(0)\|_{H_{\text{ul}}^1} + K_0 \int_0^t e^{-\Lambda_0(t-s)} \left[K_1 \eta_0 \|W(s)\|_{H_{\text{ul}}^1} + |\dot{q}(s)| \|h_\xi(\xi - q(s)) \rho_\beta(\xi)\|_{H_{\text{ul}}^1} \right] ds,$$

which due to (3.12) and $\|h_\xi(\xi - q(s)) \rho_\beta(\xi)\|_{H_{\text{ul}}^1} \leq K_0$ implies

$$(3.16) \quad \|W(t)\|_{H_{\text{ul}}^1} \leq K_0 e^{-\Lambda_0 t} \|W(0)\|_{H_{\text{ul}}^1} + 2K_0 K_1 (1 + K_0) \eta_0 \int_0^t e^{-\Lambda_0(t-s)} \|W(s)\|_{H_{\text{ul}}^1} ds$$

for $0 < t < T_{\max}$. Let

$$M(T) := \sup_{0 \leq t \leq T} e^{\Lambda t} \|W(t)\|_{H_{\text{ul}}^1},$$

where $0 \leq T \leq T_{\max}$ with $T < \infty$. Equation (3.16) gives

$$\begin{aligned} e^{\Lambda t} \|W(t)\|_{H_{\text{ul}}^1} &\leq K_0 e^{-(\Lambda_0 - \Lambda)t} \|W(0)\|_{H_{\text{ul}}^1} + 2K_0 K_1 (1 + K_0) \eta_0 \int_0^t e^{-(\Lambda_0 - \Lambda)(t-s)} e^{\Lambda s} \|W(s)\|_{H_{\text{ul}}^1} ds \\ &\leq K_0 \|W(0)\|_{H_{\text{ul}}^1} + 2K_0 K_1 (1 + K_0) \eta_0 M(T) \int_0^t e^{-(\Lambda_0 - \Lambda)(t-s)} ds, \end{aligned}$$

from which we conclude that

$$M(T) \leq K_0 \|W(0)\|_{H_{\text{ul}}^1} + \frac{2K_0 K_1 (1 + K_0) \eta_0}{\Lambda_0 - \Lambda} M(T) \leq K_0 \|W(0)\|_{H_{\text{ul}}^1} + \frac{2K_0 K_1 (1 + K_0) \hat{\eta}_0}{\Lambda_0 - \Lambda} M(T).$$

The choice (3.14) of $\hat{\eta}_0$ shows that there is a constant K_2 such that

$$\sup_{0 \leq t \leq T} e^{\Lambda t} \|W(t)\|_{H_{\text{ul}}^1} \leq K_2 \|W(0)\|_{H_{\text{ul}}^1}$$

and therefore

$$(3.17) \quad \|W(t)\|_{H_{\text{ul}}^1} \leq K_2 e^{-\Lambda t} \|W(0)\|_{H_{\text{ul}}^1}$$

for $0 \leq t \leq T$ as desired. From (3.12) and (3.17), we conclude that

$$(3.18) \quad |\dot{q}(t)| \leq 2K_1 e^{-\Lambda t} \|W(0)\|_{H_{\text{ul}}^1}$$

for $0 \leq t \leq T$. To obtain an estimate for $q(t)$, we write

$$(3.19) \quad q(t) = q(s) + \int_s^t q'(\tau) d\tau$$

and, setting $s = 0$ and using (3.18), we obtain

$$|q(t)| \leq \int_0^t |\dot{q}(s)| ds \leq 2K_1 K_2 \|W(0)\|_{H_{\text{ul}}^1} \int_0^t e^{-\Lambda s} ds \leq \frac{2K_1 K_2}{\Lambda} \|W(0)\|_{H_{\text{ul}}^1}.$$

Setting $K_3 = 2K_1 K_2 / \Lambda$, we get the desired estimate

$$(3.20) \quad |q(t)| \leq K_3 \|W(0)\|_{H_{\text{ul}}^1}$$

for $0 \leq t \leq T$.

Finally, if $T_{\max} = \infty$, then (3.17), (3.12), and (3.20) are valid for all times since the constants K_2 and K_3 do not depend upon T or η_0 . Thus, (3.18) implies that the limit $q_* = \lim_{t \rightarrow \infty} q(t)$ exists, and (3.20) shows that $|q_*| \leq K_3 \|W(0)\|_{H_{\text{ul}}^1}$. We can therefore take the limit $s \rightarrow \infty$ in (3.19) and get

$$q(t) = q_* + \int_{\infty}^t q'(\tau) d\tau,$$

which, together with (3.18), gives the estimate (3.15). ■

3.2. Establishing the necessary a priori estimates. To complete the proof of Theorem 2, it suffices to prove that, for sufficiently small $0 < \eta_0 \leq 1$, there exists a $\delta_0 > 0$ such that

$$|q(t)| + \|V(t)\|_{H_{\text{ul}}^1} \leq \eta_0$$

for all $t \geq 0$ provided $\|V(0)\|_{H_{\text{ul}}^1} \leq \delta_0$. Throughout this section, we consider initial data $q(0) = 0$ and $V(0) \in H_{\text{ul}}^1$ for which $W(0) = \rho_\beta V(0) \in H_{\text{ul}}^1$.

Proposition 3.3. *There exists a constant $\varepsilon_0 > 0$ such that, if $0 < \varepsilon \leq \varepsilon_0$ and*

$$\|v_1(0)\|_{H_{\text{ul}}^1} \leq \varepsilon^2, \quad \|v_2(0)\|_{H_{\text{ul}}^1} \leq \varepsilon, \quad \|W(0)\|_{H_{\text{ul}}^1} \leq \varepsilon^2,$$

then

$$|q(t)| + \|V(t)\|_{H_{\text{ul}}^1} \leq \left[\varepsilon + \sqrt{|\alpha|} \right]^{\frac{1}{2}}$$

for $t \geq 0$ and, in particular, $T_{\max}(\eta_0) = \infty$ for $\eta_0 > 0$ sufficiently small.

Theorem 2 follows now from Proposition 3.3. Indeed, the proposition implies that (3.13) holds for all $t > 0$ so that (3.17) and (3.20) are valid for all positive times. In the remainder of this section, we prove Proposition 3.3.

Recall that v_1 satisfies (3.3), which we write as

$$(3.21) \quad \begin{aligned} \partial_t v_1 &= \partial_\xi^2 v_1 + c \partial_\xi v_1 - (1 + c)v_1 + \tilde{\mathcal{R}}_1(\xi - q(t))\rho_\beta(\xi)^{-1}w_1 + \dot{q}(t)h_\xi(\xi - q(t)) \\ &\quad + \frac{1}{2}[c - 3h(\xi - q(t))]v_1^2 - \frac{1}{2}v_1^3 + \gamma_1 v_2^2, \end{aligned}$$

where $\tilde{\mathcal{R}}_1(\xi) = [\frac{3}{2}(1 - h(\xi)) + c][1 + h(\xi)]$ and $w_1 = \rho_\beta v_1$.

We claim that the term $\tilde{\mathcal{R}}_1(\xi - q(t))\rho_\beta(\xi)^{-1}$ is bounded in H_{ul}^1 which will allow us to control the term linear in w_1 in (3.21) using the estimate (3.17) for w_1 . To show that $\tilde{\mathcal{R}}_1(\xi - q(t))\rho_\beta(\xi)^{-1}$ is bounded, we recall that $q(t)$ is bounded on $[0, T]$ on account of (3.20), $0 < \frac{3}{2}(1 - h(\xi - q(t))) \leq 3 + c$, and

$$0 < [1 + h(y)]\rho_\beta(\xi)^{-1} = \left[1 + \tanh \frac{y}{2} \right] e^{-\beta\xi}, \quad \xi < -1,$$

is bounded, which, taken together, proves boundedness in H_{ul}^1 as claimed. Using this result, we find that there is a positive constant K_4 such that

$$\tilde{\mathcal{G}}_1(\xi, q, W) := \tilde{\mathcal{R}}_1(\xi - q)\rho_\beta(\xi)^{-1}w_1 + \dot{q}h_x(\xi - q)$$

satisfies

$$\|\tilde{\mathcal{G}}_1(\cdot, q, W)\|_{H_{\text{ul}}^1} \leq K_4 \|W\|_{H_{\text{ul}}^1}$$

for all $(q, V) = (q, \rho_\beta^{-1}W)$ with norm less than one, say. For any solution (q, V) satisfying (3.13) with η_0 as in Lemma 3.2, Lemma 3.2 then implies that

$$(3.22) \quad \|\tilde{\mathcal{G}}_1(\cdot, q(t), W(t))\|_{L_{\text{ul}}^2} \leq K_4 \|W(t)\|_{H_{\text{ul}}^1} \leq K_2 K_4 e^{-\Lambda t} \|W(0)\|_{H_{\text{ul}}^1} \leq K_2 K_4 \|W(0)\|_{H_{\text{ul}}^1}$$

for $t \in [0, T_{\max})$. In particular, we have

$$(3.23) \quad \sup_{0 \leq t < T_{\max}} \|\tilde{\mathcal{G}}_1(\cdot, q(t), W(t))\|_{L_{\text{ul}}^2} \leq \frac{1}{20K_0^2\sqrt{\pi}}$$

provided

$$(3.24) \quad \|W(0)\|_{H_{\text{ul}}^1} \leq \frac{1}{20K_0^2K_2K_4\sqrt{\pi}}.$$

Finally, the nonlinear term

$$\tilde{\mathcal{N}}_1(q, v_1) = \frac{1}{2}[c - 3h(\xi - q)]v_1^2 - \frac{1}{2}v_1^3$$

can be estimated by

$$(3.25) \quad \|\tilde{\mathcal{N}}_1(q, v_1)\|_{H_{\text{ul}}^1} \leq \frac{5}{2}\delta_1\|v_1\|_{H_{\text{ul}}^1}^2 \leq \frac{1}{2K_0}\|v_1\|_{H_{\text{ul}}^1}$$

for all $(q, v_1) \in \mathbb{R} \times H_{\text{ul}}^1$ with $|q| \leq 1$ and $\|v_1\|_{H_{\text{ul}}^1} \leq \frac{1}{5K_0}$.

Since the H_{ul}^1 -norm is invariant under translations, we may as well consider (3.21) in the laboratory frame (x, t) in which it becomes

$$(3.26) \quad \partial_t v_1 = \mathcal{A}_1 v_1 + \tilde{\mathcal{G}}_1(x - ct, q(t), W(t)) + \tilde{\mathcal{N}}_1(q(t), v_1) + \gamma_1 v_2^2,$$

where $\mathcal{A}_1 = \partial_x^2 - (1 + c)$. The coupling term $\gamma_1 v_2^2$ makes it difficult to obtain estimates for v_1 without dealing with v_2 at the same time. Thus, our goal is to compare v_1 to the solution \bar{v}_1 of the equation

$$(3.27) \quad \partial_t \bar{v}_1 = \mathcal{A}_1 \bar{v}_1 + \tilde{\mathcal{G}}_1(x - ct, q(t), W(t)) + \tilde{\mathcal{N}}_1(q(t), \bar{v}_1)$$

with initial condition

$$\bar{v}_1(x, 0) = v_1(x, 0)$$

for which estimates are easier to obtain. As a first step toward estimating \bar{v}_1 , we state the following lemma.

Lemma 3.4. *There exists a constant $K_5 > 0$ with the following property. Consider the equation*

$$(3.28) \quad \partial_t \bar{v}_1 = \mathcal{A}_1 \bar{v}_1 + G(x, t) + \tilde{\mathcal{N}}_1(q(t), \bar{v}_1),$$

where $G(x, t)$ is a given function with

$$\sup_{0 \leq t \leq T_1} \|G(\cdot, t)\|_{L_{\text{ul}}^2} < \frac{1}{20K_0^2\sqrt{\pi}}$$

for some $T_1 > 0$, and solve it with an initial condition $\bar{v}_1(0)$ with $\|\bar{v}_1(0)\|_{H_{\text{ul}}^1} \leq \frac{1}{20K_0^2}$; then the solution \bar{v}_1 of (3.28) exists for $t \in [0, T_1]$ and

$$\|\bar{v}_1(t)\|_{H_{\text{ul}}^1} \leq K_5(\|\bar{v}_1(0)\|_{H_{\text{ul}}^1} + \sup_{0 \leq s \leq T_1} \|G(\cdot, s)\|_{L_{\text{ul}}^2})$$

for $0 \leq t \leq T_1$.

Proof. Since \mathcal{A}_1 is sectorial on H_{ul}^1 (see Lemma 2.3) and the initial condition satisfies $\|\bar{v}_1(0)\|_{H_{\text{ul}}^1} \leq \frac{1}{20K_0^2}$, we see that there is a maximal number T_2 with $0 < T_2 \leq T_1$ such that the solution to the initial-value problem (3.28) exists on $[0, T_2]$ with $\|\bar{v}_1(t)\|_{H_{\text{ul}}^1} \leq \frac{1}{5K_0}$ for $t \in [0, T_2]$. We claim that $T_2 = T_1$. Indeed, the variation-of-constants formula for \bar{v}_1 reads

$$\bar{v}_1(t) = e^{\mathcal{A}_1 t} \bar{v}_1(0) + \int_0^t e^{\mathcal{A}_1(t-s)} G(\cdot, s) \, ds + \int_0^t e^{\mathcal{A}_1(t-s)} \tilde{\mathcal{N}}_1(q(s), \bar{v}_1(s)) \, ds.$$

Using Lemma 2.3 and (3.25), we obtain

$$\begin{aligned} \|\bar{v}_1(t)\|_{H_{\text{ul}}^1} &\leq K_0 e^{-t} \|\bar{v}_1(0)\|_{H_{\text{ul}}^1} + K_0 \sup_{0 \leq s \leq T_1} \|G(\cdot, s)\|_{L_{\text{ul}}^2} \int_0^t e^{-(t-s)} (t-s)^{-\frac{1}{2}} \, ds + \frac{1}{2} \sup_{0 \leq s \leq t} \|\bar{v}_1(s)\|_{H_{\text{ul}}^1} \\ &\leq K_0 e^{-t} \|\bar{v}_1(0)\|_{H_{\text{ul}}^1} + K_0 \sqrt{\pi} \sup_{0 \leq s \leq T_1} \|G(\cdot, s)\|_{L_{\text{ul}}^2} + \frac{1}{2} \sup_{0 \leq s \leq t} \|\bar{v}_1(s)\|_{H_{\text{ul}}^1} \end{aligned}$$

for $0 \leq t \leq T_2$. Using the assumptions on $\bar{v}_1(0)$ and G , we find that $\|\bar{v}_1(T_2)\|_{H_{\text{ul}}^1} \leq \frac{1}{5K_0}$ from which we conclude that $T_2 = T_1$ as claimed. The above inequality then gives

$$\sup_{0 \leq t \leq T_1} \|\bar{v}_1(t)\|_{H_{\text{ul}}^1} \leq 2K_0 \sqrt{\pi} (\|\bar{v}_1(0)\|_{H_{\text{ul}}^1} + \sup_{0 \leq t \leq T_1} \|G(\cdot, t)\|_{L_{\text{ul}}^2}),$$

which completes the proof of the lemma. ■

To apply the preceding lemma to (3.27) on the time interval $[0, T_{\text{max}})$, we need to prove that

$$\|\tilde{\mathcal{G}}_1(\cdot, q(t), W(t))\|_{L_{\text{ul}}^2} < \frac{1}{20K_0^2 \sqrt{\pi}}$$

on $[0, T_{\text{max}})$. Equation (3.23) shows that this estimate holds for any solution (q, V) that satisfies (3.13) with η_0 as in Lemma 3.2 provided $W(0)$ satisfies (3.24). In this case, we therefore have

$$(3.29) \quad \|\bar{v}_1(t)\|_{H_{\text{ul}}^1} \leq K_5(\|\bar{v}_1(0)\|_{H_{\text{ul}}^1} + K_2 K_4 \|W(0)\|_{H_{\text{ul}}^1})$$

for $t \in [0, T_{\text{max}})$.

We shall now use the preceding estimate for \bar{v}_1 to obtain estimates for v_1 on the interval $[0, T_{\text{max}})$, where T_{max} is the maximal time for which the inequality (3.13) holds for some η_0 satisfying (3.14) and for all initial conditions for which $\|V_0\|_{H_{\text{ul}}^1}$ and $\|W_0\|_{H_{\text{ul}}^1}$ are small enough.

Lemma 3.5. *Assume that $\gamma_1 \geq 0$. There are positive numbers K_7 , α_0 , and ε_0 such that the following is true for all (α, ε) with $|\alpha| < \alpha_0$ and $0 < \varepsilon < \varepsilon_0$: If $(V, W, q) = (v_1, v_2, w_1, w_2, q)$ satisfies (3.8)–(3.10) with initial data for which*

$$(3.30) \quad \|v_1(0)\|_{H_{\text{ul}}^1} \leq \varepsilon^2, \quad \|v_2(0)\|_{H_{\text{ul}}^1} \leq \varepsilon, \quad \|W(0)\|_{H_{\text{ul}}^1} \leq \varepsilon^2,$$

then the v_2 -component of the solution satisfies

$$\|v_2(t)\|_{L_{\text{ul}}^2} \leq K_7 \left[\varepsilon + \sqrt{|\alpha|} \right]^{\frac{1}{2}}$$

for all t with $0 < t < T_{\text{max}}$.

Proof. Using (3.30), we infer from (3.29) that $\|\bar{v}_1(t)\|_{C^0} \leq K_0 \|\bar{v}_1(t)\|_{H_{\text{ul}}^1} \leq K_6 \varepsilon^2$, where $K_6 = K_0 K_2 K_4 K_5$ does not depend on ε , and therefore

$$\bar{v}_1(x, t) \geq -K_6 \varepsilon^2$$

for all $x \in \mathbb{R}$ and $0 < t < T_{\text{max}}$. Next, (3.26) and (3.27) together with the assumption $\gamma_1 \geq 0$ show that

$$\begin{aligned} & \partial_t \bar{v}_1 - \mathcal{A}_1 \bar{v}_1 - \tilde{\mathcal{G}}_1(x - ct, q(t), W(t)) - \tilde{\mathcal{N}}_1(q(t), \bar{v}_1) \stackrel{(3.27)}{=} 0 \\ & \leq \gamma_1 v_2^2 \stackrel{(3.26)}{=} \partial_t v_1 - \mathcal{A}_1 v_1 - \tilde{\mathcal{G}}_1(x - ct, q(t), W(t)) - \tilde{\mathcal{N}}_1(q(t), v_1). \end{aligned}$$

The comparison principle [4, Theorem 25.1 in section VII] gives $\bar{v}_1(x, t) \leq v_1(x, t)$ for $0 \leq t < T_{\text{max}}$ and $x \in \mathbb{R}$, and therefore

$$(3.31) \quad v_1(x, t) \geq \bar{v}_1(x, t) \geq -K_6 \varepsilon^2$$

for $0 \leq t < T_{\text{max}}$ and $x \in \mathbb{R}$. Having established the lower pointwise bound (3.31) for v_1 , we return to the equation

$$\partial_t v_2 = -(1 + \partial_x^2) v_2 + \alpha v_2 - v_2^3 - \gamma_2 [1 + h(x - ct - q(t))] v_2 - \gamma_2 v_1 v_2$$

for v_2 , written in the laboratory frame. Using Lemma 2.1(iii) and the bounds (3.31), $\gamma_2 \geq 0$, and $[1 + h(y)] \geq 0$ for all $y \in \mathbb{R}$, we obtain

$$\begin{aligned} \frac{1}{2} \partial_t \|v_2\|_{L_{\text{ul}}^2(\sigma_b)}^2 & \leq \left[\frac{7}{2} b^2 + |\alpha| \right] \int_{\mathbb{R}} \sigma_b v_2^2 dx - \int_{\mathbb{R}} \sigma_b v_2^4 dx - \int_{\mathbb{R}} \sigma_b \gamma_2 [1 + h(x - ct - q(t))] v_2^2 dx \\ & \quad + \gamma_2 K_6 \varepsilon^2 \int_{\mathbb{R}} \sigma_b v_2^2 dx \\ & \leq \left[\frac{7}{2} b^2 + K_6 \gamma_2 \varepsilon^2 + |\alpha| \right] \int_{\mathbb{R}} \sigma_b v_2^2 dx - \int_{\mathbb{R}} \sigma_b v_2^4 dx. \end{aligned}$$

Next, we record that

$$\int_{\mathbb{R}} a \sigma_b v_2^2 dx - \int_{\mathbb{R}} \sigma_b v_2^4 dx \leq \frac{a^2}{b} - \int_{\mathbb{R}} a \sigma_b v_2^2 dx$$

for any constant $a > 0$ since

$$\int 2a\sigma_b v_2^2 - \int \sigma_b v_2^4 \leq \int \sqrt{2a}\sigma_b^{1/2} \sqrt{2}\sigma_b^{1/2} v_2^2 - \int \sigma_b v_2^4 \leq \int a^2 \sigma_b + \int \sigma_b v_2^4 - \int \sigma_b v_2^4 \leq \frac{a^2}{b}.$$

Therefore,

$$\frac{1}{2} \partial_t \|v_2\|_{L_{\text{ul}}^2(\sigma_b)}^2 \leq \frac{[7b^2 + 2(K_6\gamma_2\varepsilon^2 + |\alpha|)]^2}{4b} - \frac{1}{2}[7b^2 + 2(K_6\gamma_2\varepsilon^2 + |\alpha|)] \|v_2\|_{L_{\text{ul}}^2(\sigma_b)}^2.$$

This is a differential inequality of the form $\frac{1}{2}f'(t) \leq d_1 - d_2f(t)$ for which Gronwall's estimate [13, Theorem 1.5.7] gives

$$f(t) \leq e^{-2d_2t} f(0) + \frac{d_1}{d_2}(1 - e^{-2d_2t}) \leq f(0) + \frac{d_1}{d_2}$$

for $d_2 > 0$. In our case, this estimate becomes

$$\|v_2(t)\|_{L_{\text{ul}}^2(\sigma_b)}^2 \leq \|v_2(0)\|_{L_{\text{ul}}^2(\sigma_b)}^2 + \frac{7b^2 + 2(K_6\gamma_2\varepsilon^2 + |\alpha|)}{2b} \leq \frac{2K_0^2\varepsilon^2 + [7b^2 + 2(K_6\gamma_2\varepsilon^2 + |\alpha|)]}{2b},$$

where we used that

$$\|v_2(0)\|_{L_{\text{ul}}^2(\sigma_b)}^2 \leq \frac{1}{b} \|v_2(0)\|_{L_{\text{ul}}^2(\sigma)}^2 \leq \frac{K_0^2}{b} \|v_2(0)\|_{H_{\text{ul}}^1}^2 \leq \frac{K_0^2\varepsilon^2}{b}.$$

Setting $b = \sqrt{\varepsilon^2 + |\alpha|}$ and using Lemma 2.1(ii), we finally get

$$\|v_2(t)\|_{L_{\text{ul}}^2}^2 \leq K_7^2 \sqrt{\varepsilon^2 + |\alpha|}, \quad 0 \leq t < T_{\text{max}},$$

for an appropriate constant K_7 that depends only on $K_0, K_6,$ and γ_2 but not on $\alpha, \varepsilon,$ or t . ■

Next, we estimate v_1 and v_2 in the H_{ul}^1 -norm.

Lemma 3.6. *Assume that $\gamma_1 \geq 0$. There are positive numbers $K_8, \alpha_0,$ and ε_0 such that the following is true for all (α, ε) with $|\alpha| < \alpha_0$ and $0 < \varepsilon < \varepsilon_0$: If $(V, W, q) = (v_1, v_2, w_1, w_2, q)$ satisfies (3.8)–(3.10) with initial data for which (3.30) holds, then*

$$(3.32) \quad \|V(t)\|_{H_{\text{ul}}^1} \leq K_8 \left[\varepsilon + \sqrt{|\alpha|} \right]^{\frac{1}{2}}$$

uniformly in $t \in [0, T_{\text{max}})$.

Proof. First, we shall estimate $\|v_1\|_{H_{\text{ul}}^1}$. Assumption (3.30) allows us to apply Lemma 3.4, and we conclude

$$\|v_2(t)\|_{L_{\text{ul}}^2} \leq K_7 \left[\varepsilon + \sqrt{|\alpha|} \right]^{\frac{1}{2}}$$

on $[0, T_{\text{max}})$. Furthermore, from the definition of T_{max} , we know that $\|V(t)\|_{H_{\text{ul}}^1} \leq \eta_0$ on $[0, T_{\text{max}})$. Taken together, these estimates show that

$$(3.33) \quad \|v_2^2(t)\|_{L_{\text{ul}}^2} \leq \eta_0 K_0 K_7 \left[\varepsilon + \sqrt{|\alpha|} \right]^{\frac{1}{2}}$$

on $[0, T_{\max})$. To find an estimate for $\|v_1(t)\|_{H_{\text{ul}}^1}$, we wish to apply Lemma 3.4 to (3.26) which means that we have to set

$$G(x, t) := \tilde{\mathcal{G}}_1(x - ct, q(t), W(t)) + \gamma_1 v_2(x, t)^2$$

in Lemma 3.4. The estimates (3.22) and (3.33) give

$$\|G(\cdot, t)\|_{L_{\text{ul}}^2} \leq K_9 \left(\|W(0)\|_{H_{\text{ul}}^1} + [\varepsilon + \sqrt{|\alpha|}]^{\frac{1}{2}} \right)$$

for some constant K_9 that does not depend on α , ε , or t . Lemma 3.4 and (3.30) now show that

$$\|v_1(t)\|_{H_{\text{ul}}^1} \leq K_5 K_9 \left(\|v_1(0)\|_{H_{\text{ul}}^1} + \|W(0)\|_{H_{\text{ul}}^1} + [\varepsilon + \sqrt{|\alpha|}]^{\frac{1}{2}} \right) \leq K_5 K_9 [\varepsilon + \sqrt{|\alpha|}]^{\frac{1}{2}}$$

on $[0, T_{\max})$.

Next, we employ energy methods to estimate $\|v_2(t)\|_{H_{\text{ul}}^1}$, and we begin by collecting the bounds

$$\|V(t)\|_{H_{\text{ul}}^1} \leq \eta_0, \quad \|v_2(t)\|_{L_{\text{ul}}^2} \leq K_7 [\varepsilon + \sqrt{|\alpha|}]^{\frac{1}{2}}, \quad \|W(t)\|_{H_{\text{ul}}^1} \leq K_2 \|W(0)\|_{H_{\text{ul}}^1} \leq K_2 \varepsilon^2,$$

which we established so far on the time interval $[0, T_{\max})$. We write the equation for the v_2 -component in the form

$$\partial_t v_2 = -(1 + \partial_x^2)^2 v_2 + \alpha v_2 - v_2^3 + \mathcal{R}_2(x - ct - q(t)) \rho_\beta(x - ct)^{-1} w_2 - \gamma_2 v_1 v_2,$$

where we recall that $\mathcal{R}_2(y - q(t)) \rho_\beta(y)^{-1}$ is bounded in H_{ul}^1 , and consider also the equivalent integral equation

$$(3.34) \quad v_2(t) = e^{\mathcal{A}_2 t} v_2(0) + \int_0^t e^{\mathcal{A}_2(t-s)} [\alpha v_2(s) - v_2^3(s) - \gamma_2 v_1(s) v_2(s) + \mathcal{R}_2(x - cs - q(s)) \rho_\beta(x - cs)^{-1} w_2(s)] ds$$

with $\mathcal{A}_2 = -(1 + \partial_x^2)^2$. Lemma 2.3 shows that

$$\|e^{\mathcal{A}_2 t}\|_{H_{\text{ul}}^1} \leq K_0, \quad \|e^{\mathcal{A}_2 t}\|_{L_{\text{ul}}^2 \rightarrow H_{\text{ul}}^1} \leq K_0 t^{-\frac{1}{4}}, \quad t > 0,$$

and applying these estimates together with (3.17) to (3.34) gives

$$\begin{aligned} \|v_2(t)\|_{H_{\text{ul}}^1} &\leq K_0 \|v_2(0)\|_{H_{\text{ul}}^1} + K_0 \int_0^t (t-s)^{-\frac{1}{4}} \left[|\alpha| \|v_2(s)\|_{L_{\text{ul}}^2} + \|v_2(s)\|_{L_{\text{ul}}^2}^2 \|v_2(s)\|_{H_{\text{ul}}^1} \right. \\ &\quad \left. + \|v_1(s)\|_{H_{\text{ul}}^1} \|v_2(s)\|_{L_{\text{ul}}^2} + \|W(0)\|_{H_{\text{ul}}^1} \right] ds, \end{aligned}$$

where we used that

$$\|v_2^3\|_{L_{\text{ul}}^2} \leq K_0 \|v_2\|_{L_{\text{ul}}^2} \|v_2\|_{C^0}^2 \leq K_0^2 \|v_2\|_{L_{\text{ul}}^2}^2 \|v_2\|_{H_{\text{ul}}^1}$$

on account of Lemma 2.1(i).

We set $T_1 := \min\{T_{\max}, 1\}$. For $0 < t < T_1$, we then have

$$\|v_2(t)\|_{H_{\text{ul}}^1} \leq K_0 K_7 \left[\|v_2(0)\|_{H_{\text{ul}}^1} + \int_0^t (t-s)^{-\frac{1}{4}} \left(|\alpha| \left[\varepsilon + \sqrt{|\alpha|} \right]^{\frac{1}{2}} + \left[\varepsilon + \sqrt{|\alpha|} \right] \left[1 + \sup_{0 \leq s \leq t} \|v_2(s)\|_{H_{\text{ul}}^1} \right] \right) ds \right],$$

and therefore

$$\sup_{0 \leq t \leq T_1} \|v_2(t)\|_{H_{\text{ul}}^1} \leq K_{10} \left(\|v_2(0)\|_{H_{\text{ul}}^1} + \left[\varepsilon + \sqrt{|\alpha|} \right]^{\frac{1}{2}} + \left[\varepsilon + \sqrt{|\alpha|} \right] \sup_{0 \leq t \leq T_1} \|v_2(t)\|_{H_{\text{ul}}^1} \right)$$

for an appropriate constant K_{10} that does not depend on α , ε , or T_1 (as long as $T_1 \leq 1$). We now choose positive bounds α_0 and ε_0 for α and ε , respectively, that are so small that $K_{10}[\varepsilon_0 + \sqrt{\alpha_0}] \leq \frac{1}{2}$. For all (α, ε) with $|\alpha| < \alpha_0$ and $|\varepsilon| < \varepsilon_0$ we then have

$$\sup_{0 \leq t \leq T_1} \|v_2(t)\|_{H_{\text{ul}}^1} \leq 2K_{10} \left[\|v_2(0)\|_{H_{\text{ul}}^1} + \left[\varepsilon + \sqrt{|\alpha|} \right]^{\frac{1}{2}} \right].$$

To obtain estimates for $\|v_2(t)\|_{H_{\text{ul}}^1}$ for $t > 1$, we use the variation-of-constants formula

$$v_2(t) = e^{A_2(t-\tau)} v_2(\tau) + \int_{\tau}^t e^{A_2(t-s)} \left[\alpha v_2(s) - v_2^3(s) - \gamma_2 v_1(s) v_2(s) + \mathcal{R}_2(x - cs - q(s)) \rho_{\beta}(x - cs)^{-1} w_2(s) \right] ds$$

on $[\tau, t]$ for each τ with $t - 1 \leq \tau \leq t$. As before, we obtain

$$\|v_2(t)\|_{H_{\text{ul}}^1} \leq K_0 (t - \tau)^{-\frac{1}{4}} \|v_2(\tau)\|_{L_{\text{ul}}^2} + K_0 \int_{\tau}^t (t-s)^{-\frac{1}{4}} \left[|\alpha| \|v_2(s)\|_{L_{\text{ul}}^2} + \|w_2(s)\|_{H_{\text{ul}}^1} + \|v_2(s)\|_{L_{\text{ul}}^2}^2 \|v_2(s)\|_{H_{\text{ul}}^1} + \|v_1(s)\|_{H_{\text{ul}}^1} \|v_2(s)\|_{L_{\text{ul}}^2} \right] ds$$

and consequently

$$(3.35) \quad \|v_2(t)\|_{H_{\text{ul}}^1} \leq K_0 K_7 (t - \tau)^{-\frac{1}{4}} \left[\varepsilon + \sqrt{|\alpha|} \right]^{\frac{1}{2}} + K_0 \left[\varepsilon + \sqrt{|\alpha|} \right] \int_{\tau}^t (t-s)^{-\frac{1}{4}} \left[1 + \|v_2(s)\|_{H_{\text{ul}}^1} \right] ds.$$

Upon setting

$$\mathcal{J}_1(\tau) := \left(\int_{\tau}^{\tau+1} \|v_2(s)\|_{H_{\text{ul}}^1}^3 ds \right)^{1/3},$$

Hölder's inequality gives

$$\int_{\tau}^t (t-s)^{-\frac{1}{4}} \|v_2(s)\|_{H_{\text{ul}}^1} ds \leq \left(\int_{\tau}^t (t-s)^{-\frac{3}{8}} ds \right)^{2/3} \left(\int_{\tau}^t \|v_2(s)\|_{H_{\text{ul}}^1}^3 ds \right)^{1/3} \leq K_0 \mathcal{J}_1(\tau),$$

and therefore

$$(3.36) \quad \left(\int_{\tau}^{\tau+1} \left[\int_{\tau}^t (t-s)^{-\frac{1}{4}} \|v_2(s)\|_{H_{\text{ul}}^1} ds \right]^3 dt \right)^{\frac{1}{3}} \leq K_0 \mathcal{J}_1(\tau).$$

Upon raising (3.35) to the power three, integrating both sides over $t \in [\tau, \tau + 1]$, taking the third root, and using (3.36), we see that

$$\mathcal{J}_1(\tau) \leq K_{11} \left([\varepsilon + \sqrt{|\alpha|}]^{\frac{1}{2}} + [\varepsilon + \sqrt{|\alpha|}] \mathcal{J}_1(\tau) \right)$$

for an appropriate constant K_{11} that does not depend on t or τ . Making α_0 and ε_0 smaller if necessary, we conclude that

$$\mathcal{J}_1(\tau) \leq 2K_{11} [\varepsilon + \sqrt{|\alpha|}]^{\frac{1}{2}},$$

and using this estimate in (3.35), we finally obtain the pointwise estimate

$$\|v_2(\tau + 1)\|_{H_{\text{ul}}^1} \leq K_0 K_{11} [\varepsilon + \sqrt{|\alpha|}]^{\frac{1}{2}},$$

which is valid for any $\tau > 0$. This completes the proof of the lemma. \blacksquare

We are now ready to complete the proof of Proposition 3.3.

Proof of Proposition 3.3. For sufficiently small $\varepsilon > 0$, Lemma 3.6 shows that $|q(t)| + \|V(t)\|_{H_{\text{ul}}^1} \leq \frac{1}{2}\eta_0$ for $0 \leq t < T_{\max}$, which contradicts the maximality of T_{\max} (see (3.13)) if T_{\max} is finite. Thus, (3.13) holds for any t , which in turn implies that (3.17) and (3.20) are valid for all times. Therefore, (3.32) holds with $T_{\max} = \infty$, which completes the proof of Proposition 3.3. \blacksquare

4. Implications of nonlinear stability and comparison with simulations. Throughout this section, we consider the system

$$(4.1) \quad \begin{aligned} \partial_t u_1 &= \partial_{\xi}^2 u_1 + c \partial_{\xi} u_1 + \frac{1}{2}(u_1 - c)(1 - u_1^2) + \gamma_1 u_2^2, \\ \partial_t u_2 &= -(1 + \partial_{\xi}^2)^2 u_2 + c \partial_{\xi} u_2 + \alpha u_2 - u_2^3 - \gamma_2 u_2(1 + u_1) \end{aligned}$$

exclusively in the frame $\xi = x - ct$ that moves with the front. In this frame, the front solution is stationary and is given by

$$U_h(\xi) = \begin{pmatrix} \tanh(\xi/2) \\ 0 \end{pmatrix}.$$

We shall also assume that the coefficients appearing in (4.1) satisfy the assumptions required in Theorem 2. This theorem then asserts that, for any function V_0 for which $\|V_0\|_{H_{\text{ul}}^1}$ is sufficiently small, the solution $U(\xi, t)$ with initial data $U(\cdot, 0) = U_h + V_0$ can be written as $U(\xi, t) = U_h(\xi - q(t)) + V(\xi, t)$ and that there is a number q_* so that

$$(4.2) \quad \|\rho_{\beta}(\cdot)V(\cdot, t)\|_{H_{\text{ul}}^1} + |q(t) - q_*| \leq K e^{-\Lambda_* t}, \quad \|V(\cdot, t)\|_{H_{\text{ul}}^1} \leq K \left[\|V_0\|_{H_{\text{ul}}^1} + \sqrt{|\alpha|} \right]^{\frac{1}{2}}$$

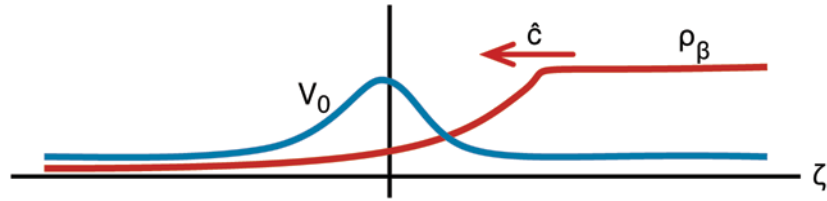


Figure 3. A schematic illustration of the interplay between the perturbation $V_0(\zeta)$ and the weight $\rho_\beta(\zeta + \hat{c}t)$ in the frame $\zeta = \xi + \hat{c}t$ that moves with the perturbation. The speed \hat{c} needs to be negative so that the weight travels to the right, since (4.3) implies that the product $\rho_\beta(\zeta + \hat{c}t)V_0(\zeta)$ tends to zero as $t \rightarrow \infty$.

for $t \geq 0$.

To see what the implications of the nonlinear stability estimates (4.2) are, let us suppose that $V(\xi, t)$ assumes the form of a traveling wave of speed \hat{c} so that $V(\xi, t) = V_0(\xi - \hat{c}t)$. Using the coordinate $\zeta = \xi - \hat{c}t$ that moves with the perturbation, we obtain from (4.2) that

$$(4.3) \quad Ke^{-\Lambda_*t} \geq \|\rho_{\beta_*}(\cdot)V(\cdot, t)\|_{H_{\text{un}}^1} = \|\rho_{\beta_*}(\xi)V_0(\xi - \hat{c}t)\|_{H_{\text{un}}^1} = \|\rho_{\beta_*}(\zeta + \hat{c}t)V_0(\zeta)\|_{H_{\text{un}}^1},$$

which implies that the speed \hat{c} needs to satisfy

$$(4.4) \quad \hat{c} \leq -\frac{\Lambda_*}{\beta_*}.$$

In particular, \hat{c} is negative, meaning that any traveling wave that exists in the wake of the stationary front U_h moves toward $\xi = -\infty$, that is, away from the front U_h ; see Figure 3 for an illustration.

One possible candidate for perturbations of traveling wave type in the wake of the front U_h are *Turing fronts* which, by definition, connect the spatially periodic Turing patterns U_{per} discussed in (1.4) at $\xi = -\infty$ to the unstable homogeneous rest state U_- in the wake of the front. We shall first derive an explicit estimate c^* for the maximal speed with which they can move.

The Turing patterns (1.4) have amplitude of order $\sqrt{\alpha}$, and we therefore set $\varepsilon = K\sqrt{\alpha}$ in Theorem 2 for a sufficiently large constant K . The proof of Proposition 2.2, and in particular (2.4), shows that the spectrum of the linearization \mathcal{L}_β of (4.1) about U_h in the weighted space lies to the left of the line $\text{Re } \lambda = \alpha - c\beta + 4\beta^2 + 8\beta^4$ with the exception of the translation eigenvalue at the origin. The decay rate Λ_* in Theorem 2 is chosen in Lemma 3.2: Choosing $\hat{\eta}_0 = K\sqrt{\alpha}$ allows us to set $\Lambda_* = \Lambda = K\sqrt{\alpha} - [\alpha - c\beta + 4\beta^2 + 8\beta^4]$ (we remark here that the constants K_2 and K_3 in Lemma 3.2 depend only on the value of the left-hand side of (3.14) but not on the values of Λ and $\hat{\eta}_0$). Substituting this expression for Λ_* into (4.4), we obtain

$$\hat{c} \leq \frac{K\sqrt{\alpha} + \alpha - c\beta + 4\beta^2 + 8\beta^4}{\beta} \leq -c + \frac{K\sqrt{\alpha} + \alpha + 4\beta^2 + 8\beta^4}{\beta}.$$

The minimum $4\sqrt{K}\alpha^{1/4} + O(\alpha^{3/4})$ of the right-hand side over $\beta > 0$ is achieved at $\beta = \sqrt{K}\alpha^{1/4} + O(\alpha^{3/4})$, which gives the upper bound

$$(4.5) \quad \hat{c} \leq c^* := -c + 4\sqrt{K}\alpha^{1/4} + O(\alpha^{3/4})$$

for the speed of traveling fronts with amplitude bounded by $K\sqrt{\alpha}$ to the left of the stationary front U_h . We remark that similar upper bounds for more general solutions of the Swift–Hohenberg equation, but without the presence of a front to the right, were obtained in [5].

Next, we complement the upper bound (4.5) for \hat{c} by formal lower bounds using the results in [6, 20] by van Saarloos and his collaborators who derived lower bounds c_* for the propagation of Turing patterns into the unstable homogeneous rest state U_- . Applying the formulas in [20, section 2.11] to the u_2 -component

$$\partial_t v_2 = -(1 + \partial_\xi^2)^2 v_2 + c \partial_\xi v_2 + \alpha v_2$$

of the linearization of (4.1) about $U_- = (1, 0)$, we obtain the lower bound

$$(4.6) \quad c_* = -c + 4\sqrt{\alpha} + O(\alpha^{3/2})$$

for Turing fronts. Thus, combining (4.5) and (4.6), we expect that Turing fronts in the wake of the stationary front U_h travel at a speed \hat{c} with $c_* \leq \hat{c} \leq c^*$ to the left.

In summary, Theorem 2 shows that small perturbations to the front should move away from the front at a speed \hat{c} that satisfies (4.4). If the perturbations are of order $\sqrt{\alpha}$, then the speed at which they have to move to the left satisfies the more explicit estimate (4.5). Furthermore, if we construct an initial condition that consists of the small-amplitude Turing patterns at $\xi = -\infty$ with the front U_h to their right, then we expect that the solution to (4.1) is the superposition of the stationary front U_h with a Turing front in its wake whose speed \hat{c} lies between the lower and upper bounds provided by (4.6) and (4.5), respectively. This last claim is based only on formal arguments, though.

We now compare these predictions with numerical simulations of (4.1). Throughout, we set

$$(4.7) \quad \gamma_1 = 0.5, \quad \gamma_2 = 0.6, \quad c = 0.5$$

and solve (4.1) on the interval $(0, \ell)$ for $\ell = 1000$ with the boundary conditions

$$u_1(0, t) = -1, \quad u_1(\ell, t) = 1, \quad u_2(0, t) = \partial_\xi u_2(0, t) = u_2(\ell, t) = \partial_\xi u_2(\ell, t) = 0.$$

We discretized (4.1) using centered finite differences with step size 0.05 and integrated the resulting ODE using the explicit Runge–Kutta–Chebyshev scheme developed in [27]. Throughout, we pick the initial condition

$$(4.8) \quad U_0(\xi) = \begin{pmatrix} \tanh[0.5(\xi - 950)] + 0.045 \cos \xi \\ 0.045 \cos \xi \end{pmatrix},$$

which excites the most unstable linear mode over the entire domain, and comment in section 5 on other initial data.

First, we choose $\alpha = 0.001$ to be very small in order to test the speed predictions from (4.5) and (4.6). In Figure 4, we plot the difference $V(\xi, t) = (v_1, v_2)(\xi, t)$ between the solution $U(\xi, t)$ and the front $U_h(\xi - 950.024)$ at $t = 1000$ for $\alpha = 0.001$. The relative offset 0.024 to the front interface at $\xi = 950$ for $t = 0$ minimizes the difference between U and U_h near

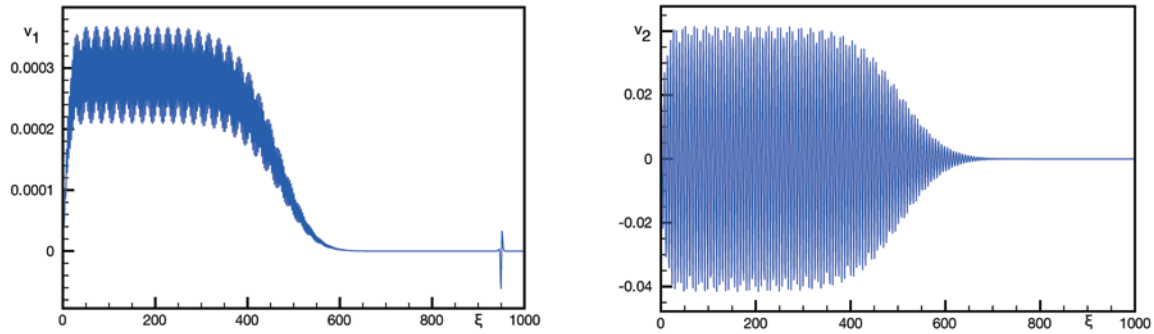


Figure 4. Plotted are the values of $v_1 = u_1 - h(\cdot - 950.024)$ (left) and of $v_2 = u_2$ (right) for $\alpha = 0.001$ in the comoving frame as functions of ξ for $t = 1000$: The Turing patterns behind the front have been pushed to the left of the front interface which is located at $\xi = 950.024$ for $t = 1000$.

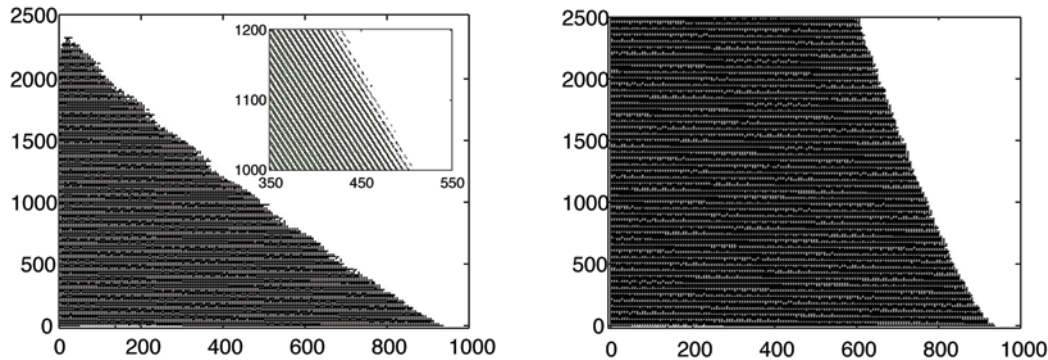


Figure 5. Space-time contour plots of $v_2 = u_2$ are shown for $\alpha = 0.001$ (left) and $\alpha = 0.01$ (right) in the comoving frame (time t upward and space ξ horizontal). The inset illustrates that small individual Turing patterns behind the front travel to the left as expected. For $\alpha = 0.001$, the overall perturbation also travels to the left at an approximately constant speed -0.384 . For $\alpha = 0.01$, the perturbation still travels to the left, but at a much smaller speed.

$\xi = 950$ and accounts therefore for the shift $q(t)$ from Theorem 2. Figure 4 indicates that V becomes very small ahead of and near the front as expected, while it develops Turing patterns to the left of the front, that is, in the spatial regime where the background state is unstable. Upon measuring the slope of the Turing front interface in the contour plot shown in Figure 5 (left plot), we find that the Turing front travels at speed -0.384 to the left. This is in agreement with the formal lower bound (4.6) which gives the minimal speed $c_* = -0.373$ upon substituting $\alpha = 0.001$ into (4.6).

For larger values α , the perturbation will still evolve into Turing fronts which are pushed to the left of the front, but the relative speed between the Turing front and the large front h will decrease as α increases. This is illustrated in the simulation for $\alpha = 0.01$ shown in the right plot of Figure 5.

Eventually, for sufficiently large parameters α , the instability of the background state $u = 0$, which is initially convective in nature, will become an absolute instability: Perturbations of the background state will then no longer be convected away but will grow in amplitude

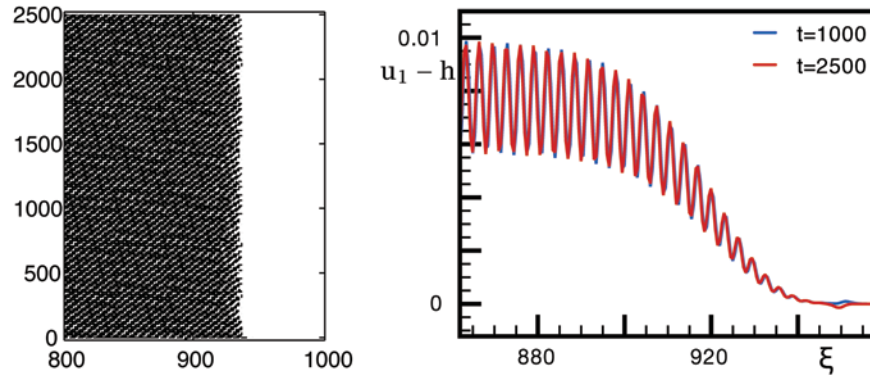


Figure 6. The simulations in this figure are for $\alpha = 0.03$. On the left, a space-time contour plot of $v_2 = u_2$ is shown in the comoving frame (time t upward and space ξ horizontal). On the right, we plotted $v_1 = u_1 - h(\cdot - 950.02)$ at $t = 1000$ in blue and $v_1 = u_1 - h(\cdot - 950.0135)$ at $t = 2500$ in red: Note that the two graphs lie on top of each other which indicates that the Turing patterns have locked to the front h .

as time increases at each fixed point in space. In this situation, we can no longer expect that perturbations will be pushed away by the front. Instead, the Turing patterns behind the front may lock to the front, yielding a time-periodic wave in an appropriate comoving frame. The convective instability changes to an absolute instability when the linear dispersion relation $\lambda = \lambda_-(k)$ from (2.3) has a double root $k_{bp} \in \mathbb{C}$ with $\lambda \in i\mathbb{R}$; see, for instance, [3] or [21] and the references therein. For our system with parameter values as in (4.7), the transition from convective to absolute instability occurs at $\alpha = 0.015$. Figure 6 shows simulations for $\alpha = 0.03$ which illustrate that the expected locking behavior between the front and the Turing pattern in its wake indeed occurs in our system.

In summary, our numerical simulations with initial data (4.8) show that the corresponding solution is indeed composed of two fronts—a Turing front which connects the Turing pattern at $-\infty$ to the unstable homogeneous rest state $U_- = (-1, 0)$, and the primary front h which connects $(-1, 0)$ to the stable homogeneous rest state $(1, 0)$ at $+\infty$. In the parameter regime where the equilibrium U_- is only convectively unstable, the relative speed between the two fronts is positive, and the front h therefore is asymptotically stable in the weighted norm as predicted by Theorem 2. As α increases, the relative speed between the two interfaces decreases. For sufficiently large α , the equilibrium U_- is absolutely unstable, and we then observe locking of the front h and the Turing pattern in its wake.

5. Discussion. In this paper, we discussed the nonlinear stability of convectively unstable fronts near supercritical Turing instabilities for the specific system (1.2). To prove nonlinear stability, we established a priori H_{ul}^1 -estimates for solutions with initial data close to the front and used these estimates to show exponential temporal decay of solutions when measured in exponentially weighted H_{ul}^1 -norms. While the second part of the proof generalizes easily to general partial differential equations, our proof of a priori estimates relies on the comparison principle and depends therefore on the special structure of our model system.

We expect nevertheless that our nonlinear stability result remains true for general partial differential equations, and there is indeed much numerical evidence that supports this belief.

For instance, the Gray–Scott system

$$\begin{aligned}\partial_t U_1 &= d_1 \partial_x^2 U_1 - U_1 U_2^2 + F(1 - U_1), \\ \partial_t U_2 &= d_2 \partial_x^2 U_2 + U_1 U_2^2 - (F + k)U_1\end{aligned}$$

is known to have Turing bifurcations, and direct numerical computations show that these are supercritical in certain parameter regions [15]. The direct numerical partial differential equation simulations in [23, section 8] show that the Gray–Scott system exhibits fronts in parts of this parameter regime which become convectively unstable at the supercritical Turing bifurcation. In particular, [23, Figures 14–15] indicate that the convectively unstable fronts are nonlinearly stable in the weighted norm.

Our results should also remain true if the homogeneous equilibrium U_- behind the front undergoes a supercritical Hopf bifurcation, rather than a Turing bifurcation. In both cases, the dynamics near U_- is captured by the complex Ginzburg–Landau equation (CGL)

$$(5.1) \quad A_t = (1 + ia)\partial_x^2 A + \alpha A - (1 + ib)|A|^2 A,$$

but the coefficients a and b vanish for Turing bifurcations, while they are generically nonzero for Hopf bifurcations. Depending on the values of the coefficients a and b , the Ginzburg–Landau equation may exhibit stable oscillatory waves or spatio-temporally complex patterns which, beyond onset, appear behind the front. Again, we expect that the front should outrun these structures in its wake, while leaving a growing spatial region behind it where the solution converges to the unstable equilibrium U_- . Sherratt [25] confirmed this picture, through a formal analysis, for fronts near supercritical Hopf bifurcations in the case when these can be described by λ - ω systems, i.e., for $a = 0$. We also refer the reader to [14, 25, 26] for numerical simulations in this setup and for applications to predator-prey systems.

The numerical simulations presented in section 4 used the initial condition (4.8) which selected a single linearly unstable spatially periodic mode. For more general initial data close to the front h , the perturbation remains small and is still pushed to the left for α near zero. The dynamics in the wake of the front may, however, be more complex and may, in particular, involve amplitude-modulated Turing patterns whose spatial periods vary over space: The evolution behind the front is, on a formal level, captured by the Ginzburg–Landau approximation (5.1). As mentioned previously, the nonlinear stability result presented here is valid independently of the particular dynamics behind the front, as long as a priori bounds for solutions are available.

As illustrated in Figure 6 in section 4, we expect that the stability properties of the front change when the equilibrium behind the front becomes absolutely unstable, since perturbations will then grow pointwise in space, rather than being convected toward $-\infty$. In our specific model problem, the Turing patterns lock to the front, and a modulated front (time-periodic in an appropriate moving coordinate frame) emerges which converges to spatially periodic patterns in its wake. In particular, the original front is no longer stable in weighted norms.

Finally, we comment on subcritical bifurcations behind the front. In this case, we cannot expect to have nonlinear stability in weighted norms since perturbations will not necessarily stay small in the wake of the front but may grow to finite amplitude. In particular, there is no

reason to believe that the solution in the wake will not strongly influence the front ahead, thus possibly precluding nonlinear stability; note though that the front may still be nonlinearly stable if conditions are right. In the system (4.1), these different behaviors can be observed: The Turing bifurcation is subcritical for parameters as in (4.7) with $\gamma_1 = -4$ or $\gamma_1 = -8$. Numerical simulations of (4.1) for $\gamma_1 = -4$ show that the solution behind the front converges to a spatially periodic pattern of finite amplitude which is again pushed away by the front, and the front therefore seems to be nonlinearly stable in weighted norms. For $\gamma_1 = -8$, on the other hand, the periodic patterns in the wake have much larger amplitude and lock to the front, which is therefore no longer nonlinearly stable.

REFERENCES

- [1] T. BRAND, M. KUNZE, G. SCHNEIDER, AND T. SEELBACH, *Hopf bifurcation and exchange of stability in diffusive media*, Arch. Ration. Mech. Anal., 171 (2004), pp. 263–296.
- [2] J. BRICMONT AND A. KUPIAINEN, *Renormalization group and the Ginzburg-Landau equation*, Comm. Math. Phys., 150 (1992), pp. 193–208.
- [3] R. J. BRIGGS, *Electron-Stream Interaction with Plasmas*, MIT Press, Cambridge, MA, 1964.
- [4] P. COLLET AND J.-P. ECKMANN, *Instabilities and Fronts in Extended Systems*, Princeton University Press, Princeton, NJ, 1990.
- [5] P. COLLET AND J.-P. ECKMANN, *A rigorous upper bound on the propagation speed for the Swift-Hohenberg and related equations*, J. Statist. Phys., 108 (2002), pp. 1107–1124.
- [6] U. EBERT AND W. VAN SAARLOOS, *Front propagation into unstable states: Universal algebraic convergence towards uniformly translating pulled fronts*, Phys. D, 146 (2000), pp. 1–99.
- [7] J.-P. ECKMANN AND G. SCHNEIDER, *Nonlinear stability of bifurcating front solutions for the Taylor-Couette problem*, ZAMM Z. Angew. Math. Mech., 80 (2000), pp. 745–753.
- [8] J.-P. ECKMANN AND G. SCHNEIDER, *Non-linear stability of modulated fronts for the Swift-Hohenberg equation*, Comm. Math. Phys., 225 (2002), pp. 361–397.
- [9] T. GALLAY, *Local stability of critical fronts in parabolic partial differential equations*, Nonlinearity, 7 (1994), pp. 741–764.
- [10] T. GALLAY, G. SCHNEIDER, AND H. UECKER, *Stable transport of information near essentially unstable localized structures*, Discrete Contin. Dyn. Syst. Ser. B, 4 (2004), pp. 349–390.
- [11] A. R. GHAZARYAN, *Nonlinear Convective Instability of Fronts: A Case Study*, Ph.D. thesis, Ohio State University, <http://www.ohiolink.edu/etd/view.cgi?osu117552079>.
- [12] D. HENRY, *Geometric Theory of Semilinear Parabolic Equations*, Lecture Notes in Math. 840, Springer-Verlag, New York, 1981.
- [13] E. HILLE, *Lectures on Ordinary Differential Equations*, Addison-Wesley, Reading, MA, 1969.
- [14] A. L. KAY AND J. A. SHERRATT, *On the persistence of spatiotemporal oscillations generated by invasion*, IMA J. Appl. Math., 63 (1999), pp. 199–216.
- [15] W. MAZIN, K. E. RASMUSSEN, E. MOSEKILDE, P. BORCKMANS, AND G. DEWEL, *Pattern formation in the bistable Gray-Scott model*, Math. Comput. Simulation, 40 (1996), pp. 371–396.
- [16] A. MIELKE AND G. SCHNEIDER, *Attractors for modulation equations on unbounded domains—existence and comparison*, Nonlinearity, 8 (1995), pp. 743–768.
- [17] K. J. PALMER, *Exponential dichotomies and Fredholm operators*, Proc. Amer. Math. Soc., 104 (1988), pp. 149–156.
- [18] A. PAZY, *Semigroups of Linear Operators and Applications to Partial Differential Equations*, Springer-Verlag, New York, 1983.
- [19] R. L. PEGO AND M. I. WEINSTEIN, *Asymptotic stability of solitary waves*, Comm. Math. Phys., 164 (1994), pp. 305–349.
- [20] W. VAN SAARLOOS, *Front propagation into unstable states*, Phys. Rep., 386 (2003), pp. 29–222.
- [21] B. SANDSTEDÉ AND A. SCHEEL, *Absolute and convective instabilities of waves on unbounded and large bounded domains*, Phys. D, 145 (2000), pp. 233–277.

- [22] B. SANDSTEDTE AND A. SCHEEL, *Spectral stability of modulated travelling waves bifurcating near essential instabilities*, Proc. Roy. Soc. Edinburgh Sect. A, 130 (2000), pp. 419–448.
- [23] B. SANDSTEDTE AND A. SCHEEL, *Essential instabilities of fronts: Bifurcation, and bifurcation failure*, Dyn. Syst., 16 (2001), pp. 1–28.
- [24] D. H. SATTINGER, *Weighted norms for the stability of travelling waves*, J. Differential Equations, 25 (1977), pp. 130–144.
- [25] J. A. SHERRATT, *Invading wave fronts and their oscillatory wakes linked by a modulated travelling phase resetting wave*, Phys. D, 117 (1998), pp. 145–166.
- [26] J. A. SHERRATT, B. T. EAGAN, AND M. A. LEWIS, *Oscillations and chaos behind predator-prey invasion: Mathematical artifact or ecological reality?*, Phil. Trans. Roy. Soc. London B, 352 (1997), pp. 21–38.
- [27] B. P. SOMMELJER, L. F. SHAMPINE, AND J. G. VERWER, *RKC: An explicit solver for parabolic PDEs*, J. Comput. Appl. Math., 88 (1998), pp. 315–326.